Journal of Biophysics and Structural Biology Vol. 3(1), pp. 1-23, January 2011
Available online at http://www.academicjournals.org/jbsb
ISSN 2141-2200 ©2011 Academic Journals

Full Length Research

EGFP-FMRP forms proto-stress granules: A poor surrogate for endogenous FMRP

Natalia Dolzhanskaya[1], Wen Xie[1], George Merz[2] and Robert B. Denman[1]*

[1]Department of Molecular Biology and New York State Institute for Basic Research in Developmental Disabilities, 1050 Forest Hill Road Staten Island, New York 10314, U.S.A.
[2]Department of Developmental Neurobiology, New York State Institute for Basic Research in Developmental Disabilities, 1050 Forest Hill Road, Staten Island, New York 10314, U.S.A.

Accepted 15 October 2010

Overexpressed autofluorescent-tagged versions of the Fragile mental retardation protein (FMRP) such as EGFP-FMRP have been used in protein-protein interaction studies and in studies of the composition, the formation and the localization of neuronal granules. However, the question of whether these molecules truly recapitulate the properties of the endogenous protein has not been addressed. Here we demonstrate that overexpressed EGFP-FMRP forms three distinct granule types based on colocalization with various marker proteins. The majority of EGFP-FMRP-containing granules are larger and more amorphous than known granule types. Consistent with this, there is only partial colocalization with stress granule or P-body markers. Nevertheless, agents such as sodium arsenite, which create endogenous stress granules and P-bodies and hippuristanol, which induces stress granule formation, drive EGFP-FMRP exclusively into stress granules. Additionally, whereas inhibiting methyl-protein formation alters the composition of endogenous FMRP-containing stress granules, we found that such treatment had little effect on the formation of EGFP-FMRP granules, or their composition. Altogether these data suggest that many overexpressed EGFP-FMRP granules represent proto-stress granules requiring external stimuli for their conversion. More importantly, the inherent heterogeneity of these granules suggests that caution should be used in extrapolating results obtained with autofluorescent-tagged surrogates of FMRP to endogenous FMRP granules.

Key words: EGFP, FMRP, stress granules, P-bodies, protein arginine methylation.

INTRODUCTION

Autofluorescent protein tags (AFPs) have been widely used as tools to study a variety of biological processes including, nervous system development (Brand, 1999), developmental abnormalities (Detrich III, 2008), neural stem cell development (Encinas and Enikolpov, 2008), localization of proteins in specific organelles (Di Giorgi et al., 1999), protein-protein interactions (Kedersha et al., 2005), protein-RNA interactions (Rackham and Brown, 2004), protein (Pierce and Vale, 1999) and mRNA trafficking (Querido and Chartrand, 2008) and membrane dynamics (Lippincott-Schwartz et al., 1999). Green fluorescent protein (GFP) and the myriad of spectral variants comprising the AFPs are relatively small proteins (Mr 27), but are much larger than many other widely used tags. As such, it is imperative to demonstrate that the AFP tag does not alter the transport, the localization or the functional properties of the protein being tagged (Lippincott-Schwartz et al., 1999). For example, Özlu et al. (2005) used RNA interference (RNAi) in combination with a TXL-1-GFP fusion to demonstrate that the

*Corresponding author. E-mail: rbdenman@yahoo.com. Tel: (718) 494-5199. Fax: (718) 494-5905.

Abbreviations: aDMA, Asymmetric dimethylarginine; **AdOx,** adenosine 2', 3'-dialdehyde; **AFPs,** autofluorescent proteins; DRG, dorsal root ganglion; **EGFP,** enhanced green fluorescence protein; **FMRP,** fragile X mental retardation protein **FRAP,** fluorescence recovery after photobleaching; **FXR1P,** fragile X related 1 mental retardation protein; **GFP,** green fluorescent protein; **Dcp1a,** decapping protein factor 1a; **eIF2,** eucaryotic initiation factor 2; **PRMT,** protein arginine methyltransferase; **RBP,** RNA binding protein; **RNA$_i$,** RNA interference; **sDMA,** symmetric dimethylarginine; **TIA1,** T-cell internal antigen 1; **tM1, tM2,** thresholded Manders coefficients.

transgene could functionally replace endogenous TXL-1 at the centrosome (Özlu et al., 2005).On the other hand, there appears to be a significant discrepancy between the localization of endogenous P58TFL with endogenous P-body markers and that of GFP-P58TFL and transfected P-body markers, suggesting that the fusion protein may not adequately mimic the endogenous form (Bloch and Nobre, 2010; Minagawa et al., 2009; Minagawa and Matsui, 2010). The fragile X mental retardation protein, FMRP, is a RNA binding protein that plays an important role in controlling translation in neurons (Bassell and Warren, 2008). Studies from a number of laboratories have demonstrated that endogenous FMRP associates with macromolecular granules in the brain, in the neurites of cultured neuronal cells and in the cell bodies of non-neuronal cells (Aschrafi et al., 2005; Didiot et al., 2008; Dolzhanskaya et al., 2006a; Dolzhanskaya et al., 2006b; Kanai et al., 2004; Xie et al., 2009). Immunofluorescence studies have shown that these granules tend to be small and not that prevalent. In contrast, AFP-tagged FMRPs have been used by a number of laboratories to assess various questions concerning neuronal granule make up and dynamics (Antar et al., 2005; Barbee et al., 2006; Castren et al., 2001; Cziko et al., 2009; Darnell et al., 2005; De Diego Otero et al., 2002; Dictenberg et al., 2008; Levenga et al., 2009; Ling et al., 2004; Pfeiffer and Huber, 2007). These granules tend to be much larger than endogenous FMRP granules and also much more prevalent in dendrites. However, the question of what type(s) of granules AFP-FMRP represents has not been adequately addressed.

Here we have examined EGFP-FMRP expression in HeLa cells using a variety of known granule marker proteins and under various conditions known to induce the formation of specific granule types or modulate their composition. Our studies demonstrate that EGFP-FMRP granules fall into at least three different functional classes, the majority of which appears to be a proto-stress granule. The implications of these results are discussed.

MATERIALS AND METHODS

Reagents

Sodium arsenite, adenosine 2', 3'-dialdehyde (AdOx) and emetine were purchased from Sigma. Hippuristanol was a kind gift from Jerry Pelletier (McGill Cancer Center, McGill University, Montreal, Quebec, Canada).

Plasmids and transfection

A mammalian expression plasmid containing an enhanced green fluorescent-FMRP fusion protein under the control of a cytomegalovirus promoter pEGFP-FMRP (Antar et al., 2004) was a kind gift of Dr. Gary Bassell (Emory University, Atlanta, GA). The parent vector, pEGFP-C2, was purchased from Clontech. Cells (3×10^5/35 mm dish) were transfected with 1 μg of plasmid DNA using Lipofectamine Plus (Invitrogen).

Proteins and antibodies

FMRP mAb-2160, which recognizes an epitope in the N-terminus of human FMRP, and normal mouse serum were purchased from Chemicon. Phospho-eIF2α pAb (Ser52) (KAP-CP131) and Hsp70c mAb (HSP-820) were obtained from StressGen. TIA1 pAb (sc-1751) and FXR1P pAb (sc-10552) were purchased from Santa Cruz. Asymmetric dimethylarginine pAb (ASYM24) and symmetric dimethylarginine pAb (SYM10) were purchased from Millipore. Dimethylarginine pAb (mRG) was obtained from CH3 Biosystems. Protein arginine methyltransferase antibody, PRMT1 was obtained from Abcam (ab70724), while PRMT3 pAb (07-256), PRMT4 pAb (AB3345), PRMT5 pAb (07-405) and PRMT7 pAb (07-639) were obtained from Millipore. hDcp1a pAb was a kind gift of J. Lykke-Andersen (University of Colorado, Boulder, CO).

Cell culture

HeLa cells were grown at 37°C in 5% CO_2 and maintained in DMEM supplemented with 10% FBS, 100 U/ml penicillin and 100 μg /ml streptomycin. In some cases, the cells were treated with 20 μM AdOx, 0.5 mM sodium arsenite, 10 μM hippuristanol, or with 10 μg/ml emetine and processed as indicated (Dolzhanskaya et al., 2006a).

Gene expression in cultured cells

Western blotting was carried out according to protocols set forth by the manufacturer for each antibody or as previously described (Dolzhanskaya et al., 2006a). For immunostaining, cells were grown on poly-L-lysine coated coverslips in the presence or absence of 20 μM AdOx and in the presence or absence of 0.5 mM sodium arsenite as indicated. The cells were fixed in 2% paraformaldehyde for 10 min and washed with PBS and then blocked in (RPMI1640 base medium, 0.05 % saponin, 0.1% sodium azide, 2% goat serum) for 30 min at room temperature. Subsequently, the cells were stained with antibodies to FMRP (1:500), TIA-1 (1:100), Hsp70 (1:300), FXR1P (1:50), hDcp1 (1:200), ASYM24 (1:100), mRG (1:150), or SYM10 (1:100) for 1 h. This was followed by incubation with Alexa Fluor secondary antibodies (1:500 dilutions) for 30 min at room temperature. Finally, the coverslips were washed in RPMI1640 base medium, 1% goat serum and mounted in buffered glycerol. Fluorescence was detected with an Eclipse 90i dual laser-scanning confocal microscope (NIKON). Images were acquired at 20 - 100× magnification. For presentation purposes the images were sometimes cropped to highlight certain points. All cropping was uniform within the particular figure.

Image analyses

Relative EGFP-FMRP granule size (pixels^2) was determined from select confocal images. Granules in each image file were defined using the threshold function in Image J (http://rsb.info.nih.gov.80/ij/). Granule areas were then calculated using the analyze particles feature. For calculations all images were taken at 40× magnification and the entire image was quantified; thereby ensuring a uniform pixel size. The circularity of the granules, 4π (area/perimeter^2), was calculated similarly. The data were then imported into Excel for subsequent analysis. For presentation, granule size distributions were all normalized to 500 particles and the normalized distributions were compared using the F-test for two sample variance. Protein co-localization measurements were performed by counting single- and double-stained granules of acquired images (Thomas et al., 2004). Co-localization was determined using the JaCoP Plugin (Bolte and Cordelieres, 2006; Didiot et al., 2008).

Line scans of the cellular fluorescence intensity (Biron et al., 2004) were also acquired using Image J software.

FRAP

Fluorescence recovery after photobleaching (FRAP) was measured with modification (Wang et al., 2008). HeLa cells were cultured on 40 mm coverslips and transfected with pEGFP–FMRP. Twenty four hours the cells were mounted in Sykes-Moore chambers (Bellco Glass Inc., Vineland, NJ) on a Nikon 90i microscope coupled to a Nikon C1 three-laser scanning confocal system (NIKON Instruments Inc., Melville, NY). The cells were maintained at 37°C with an air curtain incubator (NevTek, Williamsville, Va). Baseline images of EGFP-FMRP-expressing cells were acquired and select regions of interest (ROI) within the transfected cells were bleached to 10% or less of their initial intensity with the argon laser. Time-lapse images of the recovery were obtained at 30 s intervals.

Image data before and after bleaching was first concatenated and then converted into animated GIF files and processed using Image J software. The mean fluorescence within select bleached and control ROI was obtained using the analyze particles function, while fluorescence of particular EGFP–FMRP granules was measured using the linescan feature. Data were exported into Microsoft Excel for subsequent analysis. In some cases, cells were treated with arsenite 0.5 mM for 2 min prior to bleaching to induce stress granules. Arsenite was maintained throughout the 20 min FRAP time-lapse. A total of five arsenite-treated cells and five untreated cells were examined.

RESULTS

EGFP-FMRP expression results in a heterogeneous array of granules

Fluorescence microscopy of primary hippocampal neurons and Neuro 2A cells transfected with a plasmid encoding an EGFP-FMRP fusion protein has shown that its expression was in the form of granules that were confined largely to the cytoplasm (Antar et al., 2004; Darnell et al., 2005; Pfeiffer and Huber, 2007). Here, we show that HeLa cells transfected with the same plasmid express fluorescent granules with an assortment of sizes. In contrast, transfection of the parent vector shows that EGFP exhibits diffuse, non-granular cytoplasmic expression, Figure 1a. Analysis of the distribution of EGFP-FMRP granules reveals that they fall into three different size categories (small, intermediate and large), Figure 1b. In contrast, endogenous FMRP granules were much more homogeneous and mainly correspond in size to the smaller size EGFP-FMRP granules, Figure 1c. These data are consistent with two competing hypotheses. One possibility is that individual EGFP-FMRP granules have disparate compositions and possibly differing functions. The other likelihood is that the population of EGFP-FMRP granules represents nascent core particles of the same composition, but with differing aggregation states.

EGFP-FMRP expression and stress granule markers

Previous studies have shown that endogenous FMRP forms a variety of granule types including stress granules. Stress granules can be formed in response to heat shock (Mazroui et al., 2002), oxidative stress (Thomas et al., 2004), RNA binding protein over expression (Solomon et al., 2007), expression of a phosphomimetic mutant form of eukaryotic initiation factor 2 (eIF-2) (McEwen et al., 2005) and interfering with eIF4A activity (Mazroui et al., 2006). To determine whether the granules formed by expression of EGFP-FMRP were stress granules, HeLa cells were transiently transfected with an EGFP-FMRP expression vector. Twenty four hours later the cells were immunostained with anti-TIA1, an RNA binding protein which detects core stress granules (Kedersha et al., 2005) and then visualized by confocal microscopy. As shown in Figure 2a (panel a), punctate EGFP-FMRP expression was observed in the HeLa cell cytoplasm. In contrast, but as expected, TIA1 was found in both the cytoplasm and the nucleus, Figure 2a (panels b and e). In the cytoplasm TIA1 and EGFP-FMRP co-localized in large perinuclear granules; however, there were a host of EGFP-FMRP granules that did not contain TIA1. Nevertheless, it did not appear that granule size was a determining factor in the co-localization of TIA1 and EGFP-FMRP, rather there appeared to be cells with extensive co-localization, and cells with poor co-localization (Figure 2a; panels c and f) and Figure 2b. However, overall cells exhibiting extensive colocalization were in the minority. In these latter cells, TIA1 was largely found in the nucleus. Interestingly, treating cells with either hippuristanol, or arsenite, which induces stress granule formation resulted in a marked increase in the colocalization of EGFP-FMRP and TIA1, Figure 2a (panel i).

To quantify the overall extent of colocalization between EGFP-FMRP and TIA1 in the transfected HeLa cells we performed colocalization analyses. By manually masking nuclear staining and setting threshold limits on each fluorescence channel we were able to differentiate granular versus non-granular staining. Table 1 shows the thresholded Manders coefficients tM1 (fraction of red in the green channel) and tM2 (fraction of green in the red channel) for the EGFP-FMRP granules under different conditions. In the absence of treatment the majority of EGFP-FMRP granules were devoid of TIA1; however, following treatment with either sodium arsenite or hippuristanol there was a significant shift of TIA1 into these granules.

We next examined colocalization between EGFP-FMRP granules and another stress granule marker, FXR1P. Endogenous FXR1P extensively colocalizes with endogenous FMRP in arsenite-induced stress granules (Dolzhanskaya et al., 2006a, 2006b) these data are recapitulated in Figure 3a. However, as shown in Figure 3b (panels d-f), colocalization between EGFP-FMRP granules and FXR1P was also incomplete. Again however, in the presence of arsenite EGFP-FMRP granules almost completely colocalized with FXR1P, Figure 3c (panel i).

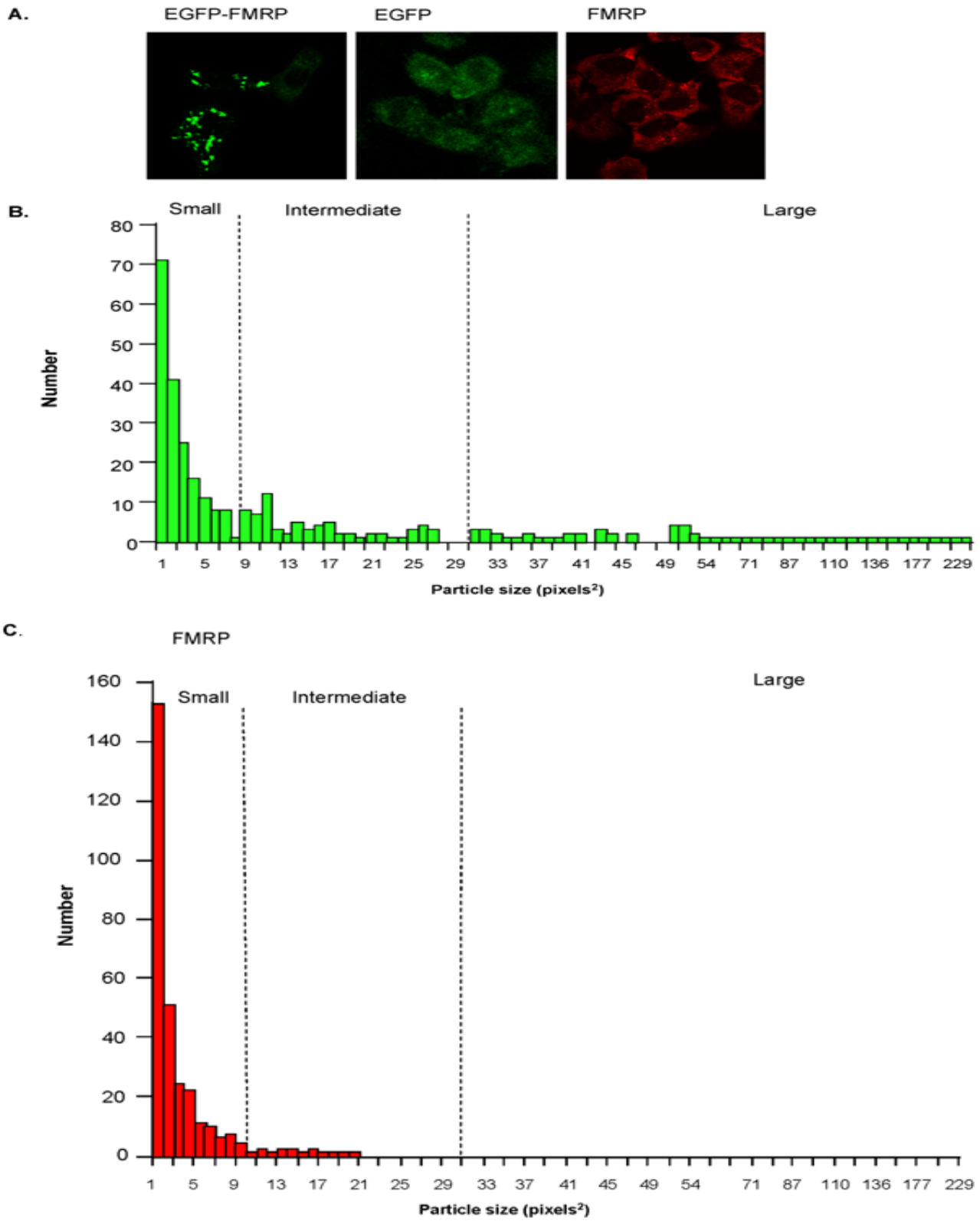

Figure 1. EGFP-FMRP granules are heterogeneous. (A) Confocal images of HeLa cells expressing EGFP-FMRP, EGFP, or endogenous FMRP. (B) Size distribution of EGFP-FMRP granules in HeLa cells. Analysis was based on 9 transfected cells. Note the three classes of granules (small, intermediate, large) based on size. (C) Size distribution of endogenous FMRP granules. Analysis was based on 27 cells. Comparison of the two distributions shows that endogenous FMRP granules are significantly smaller ($P < 0.00084$).

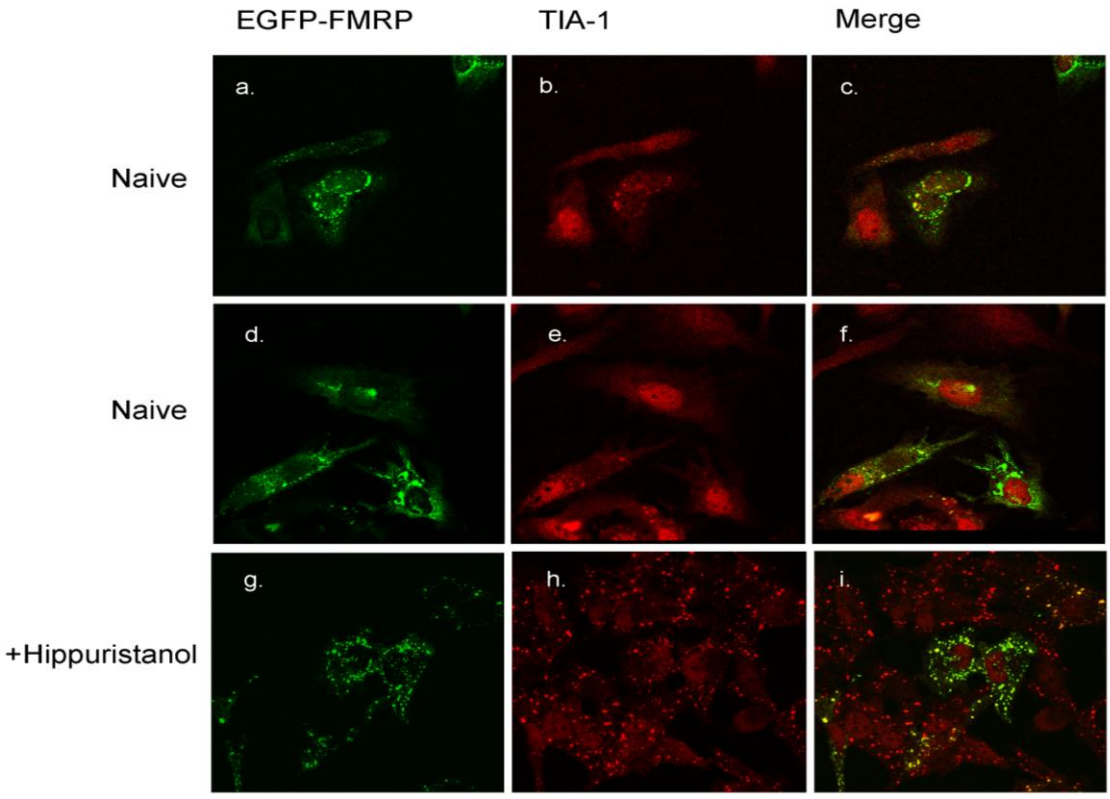

Figure 2A. EGFP-FMRP granules partially colocalize with the stress granule marker TIA1. (A) Panels a-f show EGFP-FMRP (green), TIA1 (red) and merged images of transfected HeLa cells. Panels g-i show cells treated with 10 μM hippuristanol for 30 min. Notice that all of the cells contain TIA1 stress granules (red).

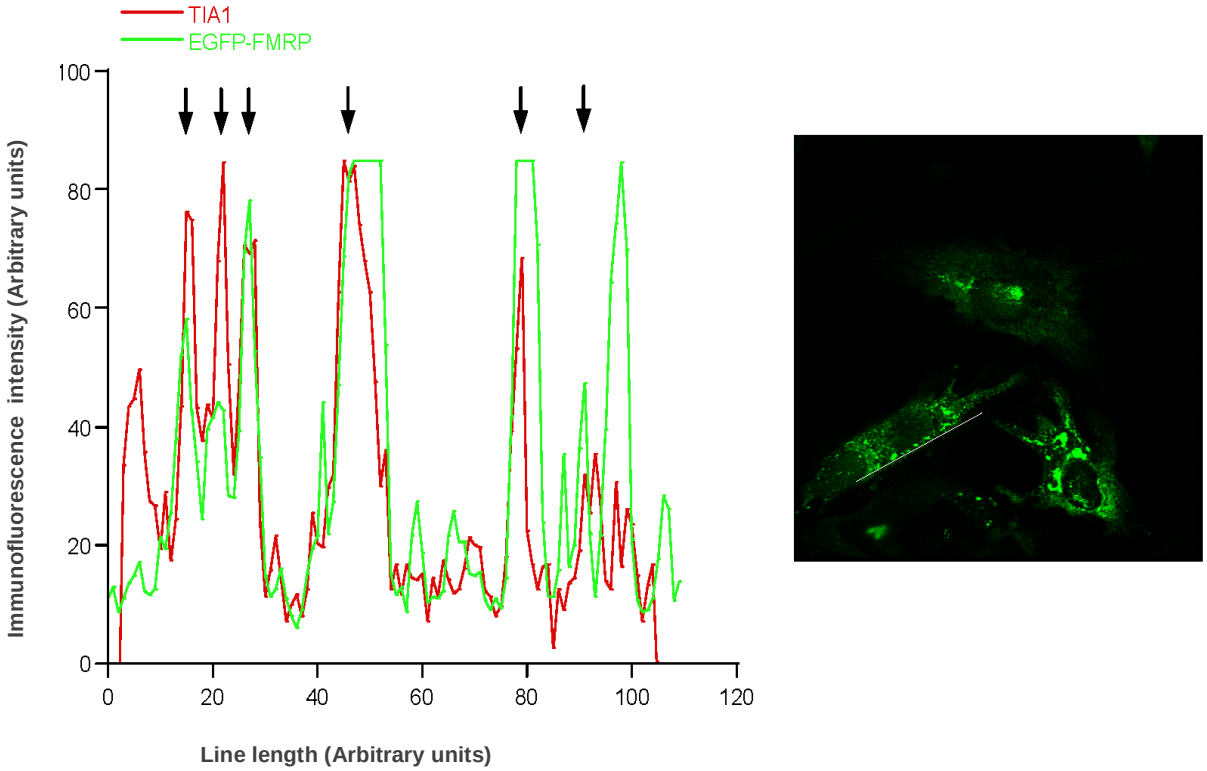

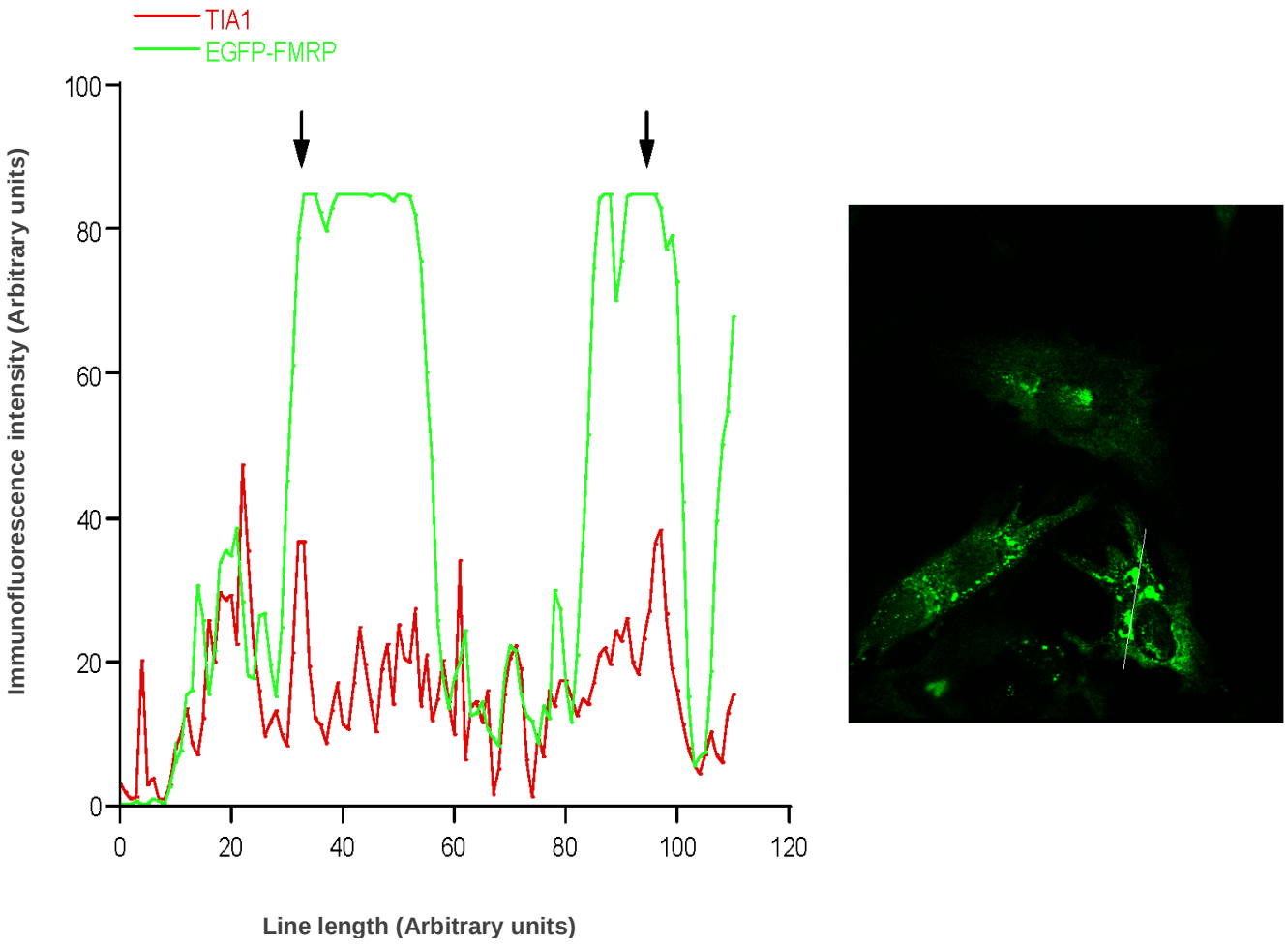

Figure 2. (B) Linescans of the red and green fluorescent channels were acquired from untreated HeLa cells expressing EGFP-FMRP and immunostained with TIA1 (Figure 1A) in which there was good colocalization of the two proteins (upper panel) or poor colocalization of the two proteins (lower panel). The arrows mark the individual EGFP-FMRP granules. The granules that were scanned are marked by a white line on the images shown to the right of the graphs.

Table 1. EGFP-FMRP colocalization analysis.

Pair	Treatment	tM1[d]	tM2[d]
EGFP-FMRP/TIA1	None	0.069 (0.015)	0.057 (0.021)
	AdOx[a]	0.068 (0.023)	0.061 (0.007)
	Arsenite[b]	0.521 (0.014) †	0.449 (0.027) †
	Hippuristanol[c]	0.228 (0.028) †	0.373 (0.003) †
EGFP-FMRP/Dcp1a	None	0.024 (0.014)	0.007 (0.003)
	AdOx[a]	0.029 (0.011)	0.006 (0.003)
	Arsenite[b]	0.028 (0.003)	0.010 (0.005)
	Hippuristanol[c]	0.111 .045) †	0.126 (0.047) †

a. HeLa cells treated with 10 μM AdOx for 24 h prior to analysis. b. HeLa cells treated with 0.5 mM sodium arsenite for 20 min prior to analysis. c. HeLa cells treated with 10 μM hippuristanol for 30 min. prior to analysis. d. Thresholded Manders coefficients (Bolte and Cordelieres, 2006) for EGFP-FMRP granules, tM1 and tM2 were calculated using the JaCoP module in Image J. The means and standard deviations, shown in parentheses, for at least 25 transfected cells per treatment are presented; fluorescence from non-transfected cells in the field was manually masked in order to examine only the colocalization of EGFP-FMRP transfected cells. †Treatment is significantly different from non-treated (P > 0.005, ANOVA).

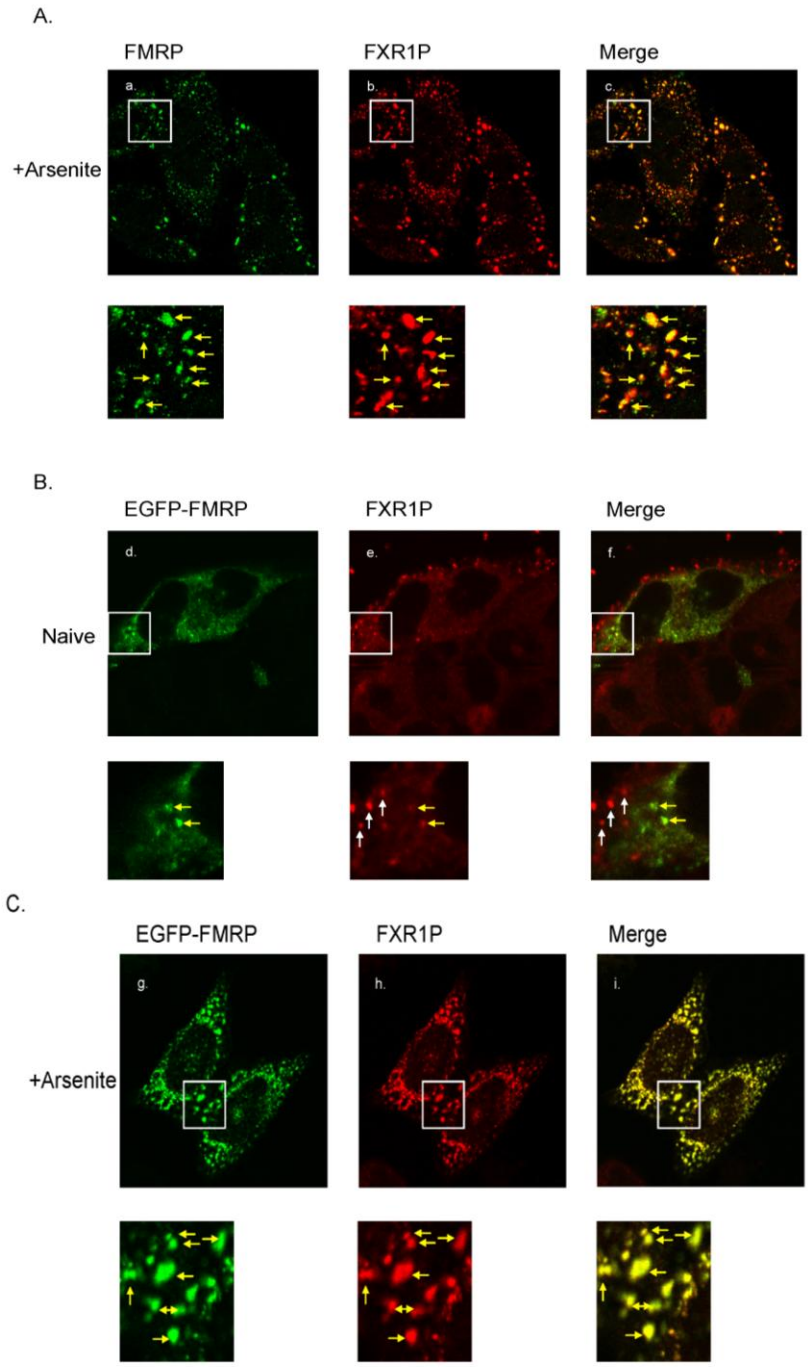

Figure 3. EGFP-FMRP granules partially colocalize with the stress granule marker FXR1P. (A) Panels a-c show endogenous FRMP (green), endogenous FXR1P (red) and merged images of HeLa cells treated with 0.5 mM arsenite for 20 minutes. Boxed areas show magnified views of select FMRP granules reveal the near complete colocalization of the granules. (B) Panels d-f show EGFP-FMRP (green), endogenous FXR1P (red) and merged images of transfected HeLa cells. Boxed areas show magnified views of select EGFP-FMRP granules. White arrows mark FXR1P-only granules; yellow arrows mark colocalized granules and green arrows mark EGFP-FMRP-only granules. (C) Panels g-i show EGFP-FMRP (green), endogenous FXR1P (red) and merged images of transfected HeLa cells treated with 0.5 mM arsenite for 20 min, 24 h post-transfection. Boxed areas show magnified views of select EGFP-FMRP granules. White arrows mark FXR1P-only granules; yellow arrows mark colocalized granules and green arrows mark EGFP-FMRP-only granules.

EGFP-FMRP granules and the P-body marker Dcp1a

P-bodies are another type of granule, distinct from, but associated with stress granules (Anderson and Kedersha, 2006). Studies have shown that certain proteins shuttle between stress granules and P-bodies, while others do not, marking them as core constituents (Kedersha et al., 2005). The decapping factor, Dcp1a, is a core constituent of P-bodies (Cougot et al., 2004). To determine whether EGFP-FMRP was associated with P-bodies HeLa cells were transiently transfected with an EGFP-FMRP expression vector. Twenty four hours later the cells were immunostained with anti-Dcp1a and visualized by confocal microscopy. Figure 4a (panel c) shows that EGFP-FMRP granules occasionally completely overlap with Dcp1a-containing granules, indicating that a portion of EGFP-FMRP was present in P-bodies. Quantitative colocalization analyses revealed however, that like the stress granule markers, the extent of colocalization was very weak, Table 1. Treating cells with sodium arsenite for 20 min following transfection produces stress granules and P-bodies (Kedersha et al., 2007). Under these conditions Dcp1a granules associate more closely with EGFP-FMRP granules, although they generally do not completely overlap, Figure 4b (panel f) and Table 1.

Thus, exogenously expressed EGFP-FMRP sorts into at least three granule types: stress granules, P-bodies and a unique granule, which represents the largest fraction of this set.

The physical characteristics of EGFP-FMRP granules differ from stress granules and P-bodies

To further characterize EGFP-FMRP granules we undertook morphometric analyses of two readily quantifiable features, granule shape and granule size. The results were compared to arsenite-induced TIA1 granules, hippuristanol-induced TIA1 granules and endogenous Dcp1a-containing P-bodies. As expected, we found that the Dcp1a-containing P-bodies were significantly smaller than arsenite-induced stress granules, hippuristanol-induced stress granules, and EGFP-FMRP granules. On the other hand, EGFP-FMRP granules were both substantially larger and more amorphous than the other granules, Table 2. These data again highlight differences between EGFP-FMRP granules and other known granule types.

The dynamic properties of EGFP-FMRP granules mimic stress granules

Emetine inhibits protein synthesis elongation (Gay et al., 1989; Grollman and Huang, 1976; Yamasaki et al., 2007) altering the dynamic equilibrium between polyribosomes and stress granules. It was found that in DU-145 cells treated with arsenite the addition of emetine at concentrations that inhibit protein synthesis effectively "dissolved" TIA1-containing stress granules (Kedersha et al., 2000). Therefore, we used emetine to assess the dynamic interrelationship between EGFP-FMRP-containing granules and polyribosomes. We first demonstrated that endogenous TIA1 stress granules and endogenous FMRP stress granules in HeLa cells treated with arsenite are substantially altered by emetine, Figure 5a. Specifically, the sizes of the granules in the emetine-treated cells were much smaller than the arsenite-induced stress granules (Figure 5b and c). We then applied this paradigm to assess the effect of emetine on EGFP-FMRP granules. Here we found that both untreated EGFP-FMRP granules and arsenite-treated EGFP-FMRP granules responded to emetine in much the same way as TIA1 and FMRP stress granules (Figure 6a, b and c).

Fluorescence recovery after photobleaching is a method that is often used to characterize the dynamic properties of granules (Kedersha et al., 2005, 2008). For example, Antar et al. (2005) examined the effect nocodazole had on EGFP-FMRP granules in cultured hippocampal neurons and found their transport within dendrites was microtubule-dependent. Here, a similar analysis was performed on EGFP-FMRP granules comparing them to ones formed following arsenite treatment. In the absence of treatment EGFP-FMRP granules exhibited a range of motilities. Some granules were quite stationary, while others were highly mobile. FRAP analysis of EGFP-FMRP transfected HeLa cells in the absence of treatment revealed that the EGFP-FMRP granules recovered 50% of their unbleached intensity within 10 min, implying that there is a dynamic exchange between non-granular EGFP-FMRP and the granules, Figure 7a, b and c. To determine whether conditions that induce the formation of stress granules alters the recovery of EGFP-FMRP granules, HeLa cells were treated with arsenite and FRAP was performed on the resulting perinuclear granules. The results showed that the treatment increased the rate of recovery slightly, but not significantly, Figure 7d.

EGFP-FMRP granules contain methylated proteins, but do not require methylated proteins for their formation

Previously we showed that endogenous FMRP-containing stress granules contain asymmetric dimethylarginine-modified proteins (aDMA-proteins) and that the cell's methylation state affected their composition (Dolzhanskaya et al., 2006a). To examine whether EGFP-FMRP granules contained asymmetrically dimethylated (aDMA) proteins HeLa cells, transiently expressing EGFP-FMRP, were incubated in the absence

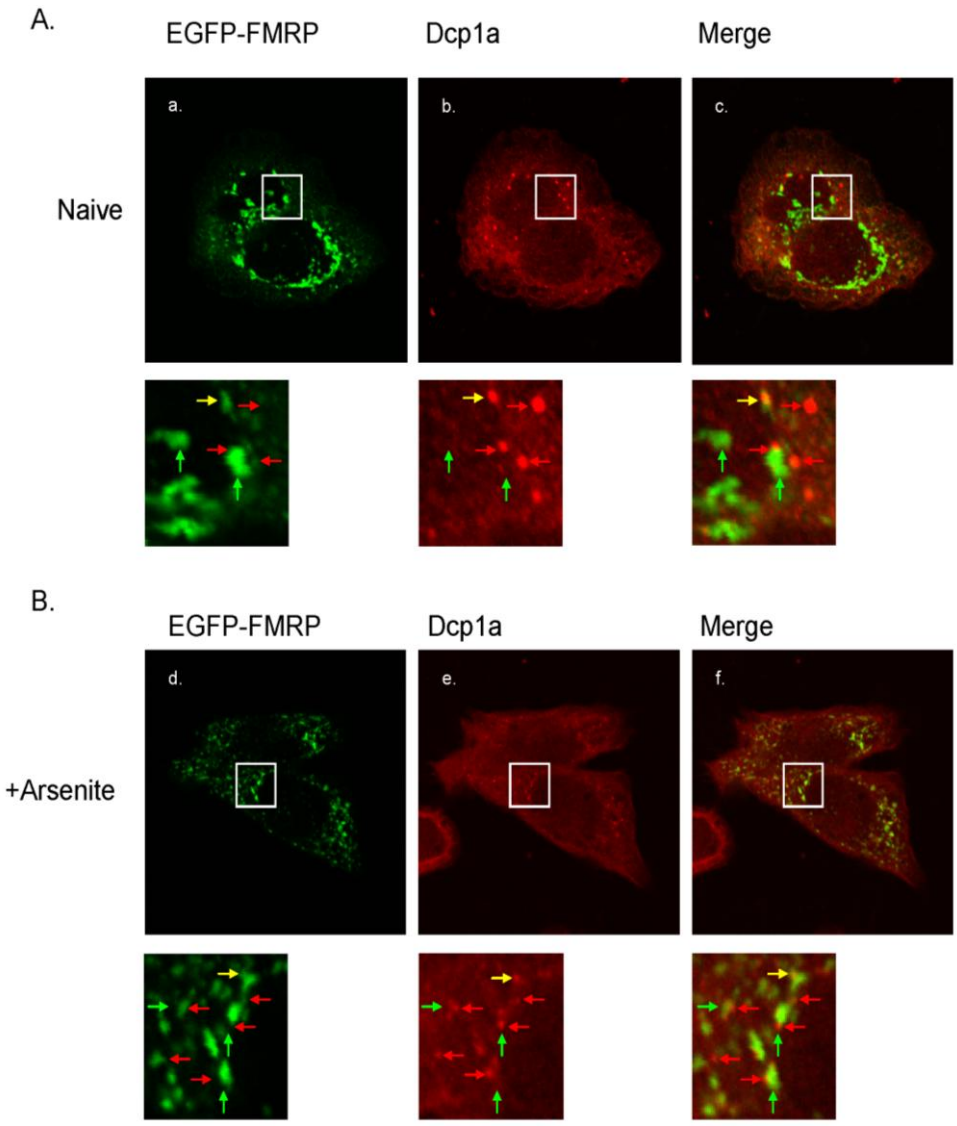

Figure 4. EGFP-FMRP granules weakly colocalize with the P-body marker protein Dcp1a. (A) Panels a-c show EGFP-FMRP (green), Dcp1a (red) and merged images of transfected untreated HeLa cells. Boxed areas presented below show magnified views of select EGFP-FMRP granules. Red arrows mark Dcp1a-only granules; yellow arrows mark colocalized granules and green arrows mark EGFP-FMRP-only granules. (B) Panels d-f show comparable images of transfected HeLa cells treated with 0.5 mM arsenite for 20 min, 24 h post-transfection. Boxed areas presented below show magnified views of select EGFP-FMRP granules. Red arrows mark Dcp1a-only granules; yellow arrows mark colocalized granules and green arrows mark EGFP-FMRP-only granules.

Table 2. Physical characteristics of EGFP-FMRP granules.

Measure/granule	EGFP-FMRP	Stress granules[c]	Stress granules[d]	P-bodies[e]
Circularity[a]	0.87 (0.2)[†]	0.91 (0.15)	0.91 (0.14)	0.95 (0.13)
Area[b]	16.2 (47) [‡]	13.8 (29)	14.4 (19)	4.4 (8)

a. Circularity measures the deviation of the granule from a perfect circle, scored as 1; the mean and (standard deviation) are shown. b. Area is given in squared pixels; the mean and (standard deviation) are shown. c. HeLa cell arsenite-induced TIA1 granules. d. HeLa cell hippuristanol-induced TIA1 granules.e. HeLa cell endogenous Dcp1a granules.† Circularity of 1000 EGFP-FMRP granules was significantly different from that of 1000 arsenite-induced granules, hippurstanol-induced granules and 1200 endogenous P-bodies ($P < 1 \times 10^{-32}$, ANOVA). ‡ Area of 1000 EGFP-FMRP granules was significantly different from that of 1000 arsenite-induced granules, 1000 hippuristanol-induced granules and 1200 endogenous P-bodies ($P < 6 \times 10^{-19}$, ANOVA).

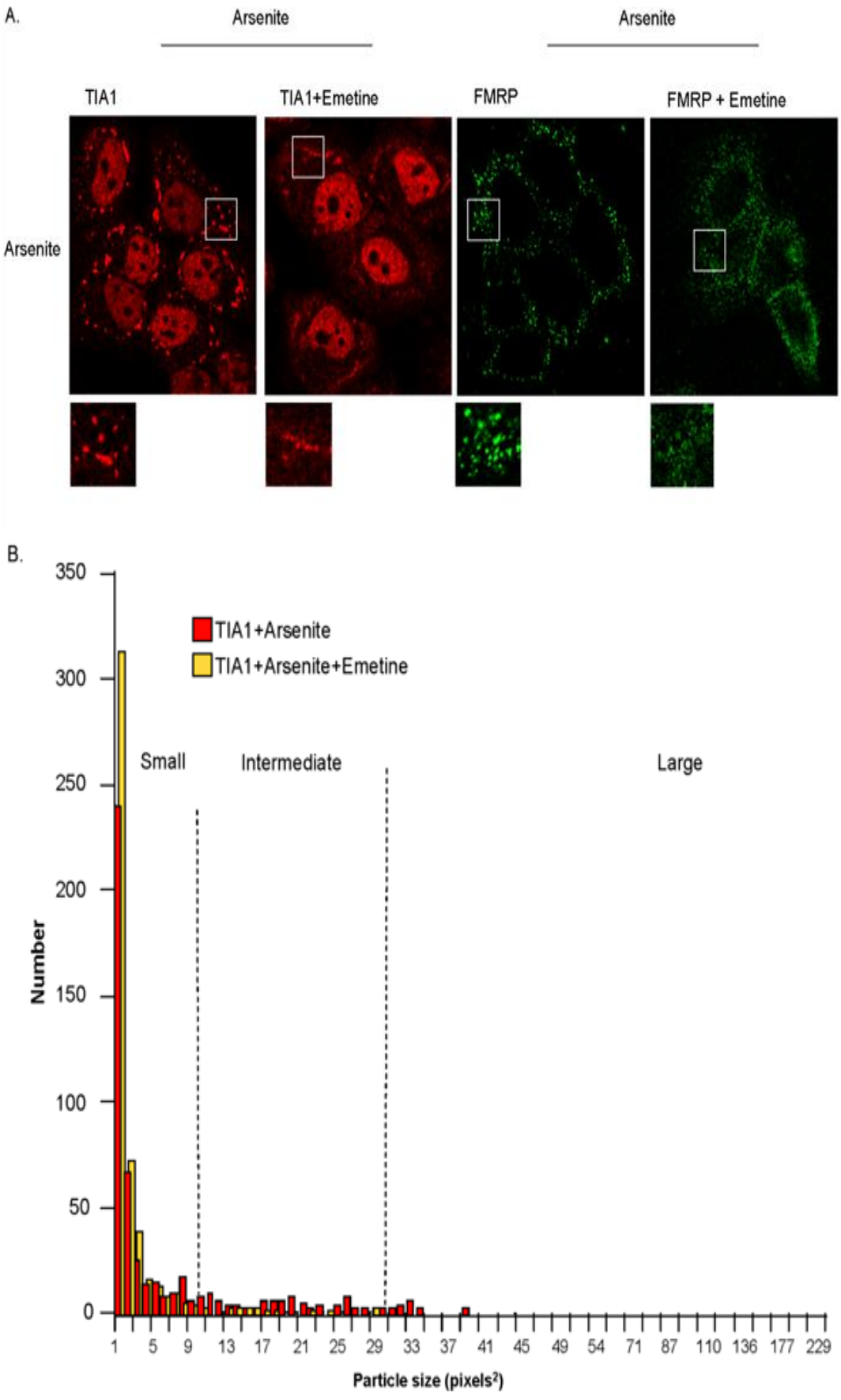
A.
Arsenite
Arsenite
TIA1
TIA1+Emetine
FMRP
FMRP + Emetine
Arsenite
B.
TIA1+Arsenite
TIA1+Arsenite+Emetine
Small
Intermediate
Large
Number
350
300
250
200
150
100
50
0
1
5
9
13
17
21
25
29
33
37
41
45
49
54
71
87
110
136
177
229
Particle size (pixels²)

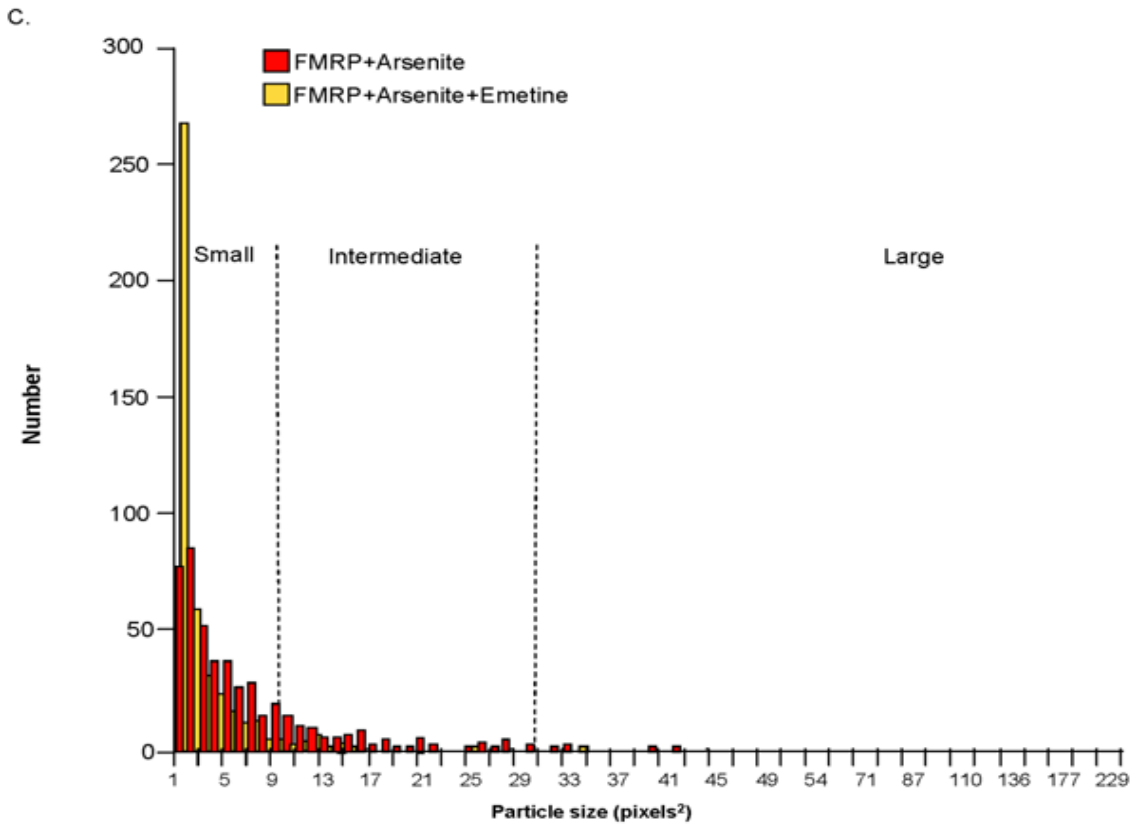

Figure 5. Endogenous TIA1 and endogenous FMRP stress granules respond to emetine. (A) Panels a-d show endogenous TIA1 (red), endogenous FMRP (green) HeLa cells treated with 0.5 mM arsenite for 20 min or treated with 0.5 mM arsenite and then 10 μg/ml of emetine for 1 h. Boxed areas presented below show magnified views of select stress granules. Size distribution of HeLa cell endogenous (B) TIA1 (C) endogenous FMRP stress granules in the presence and absence of emetine. Analysis was based on 10 cells for each protein. Comparison of the two distributions shows that emetine significantly reduces the size of both classes of stress granules ($P < 0.049$ and $P < 4.5 \times 10^{-6}$, respectively, F-test for two sample covariance).

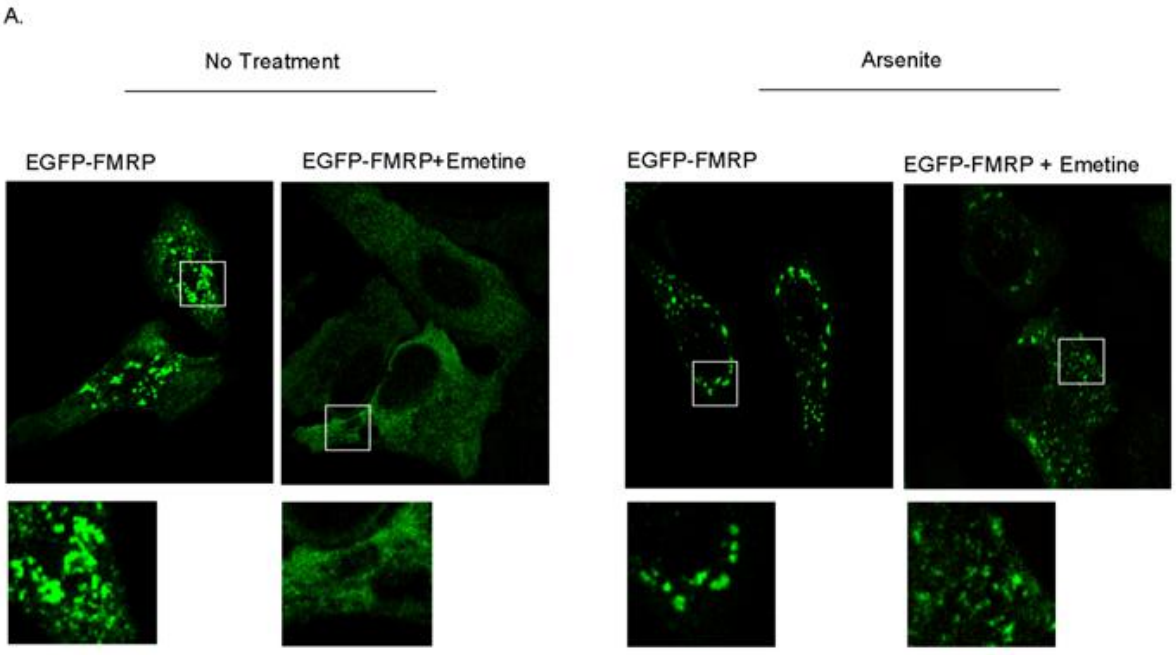

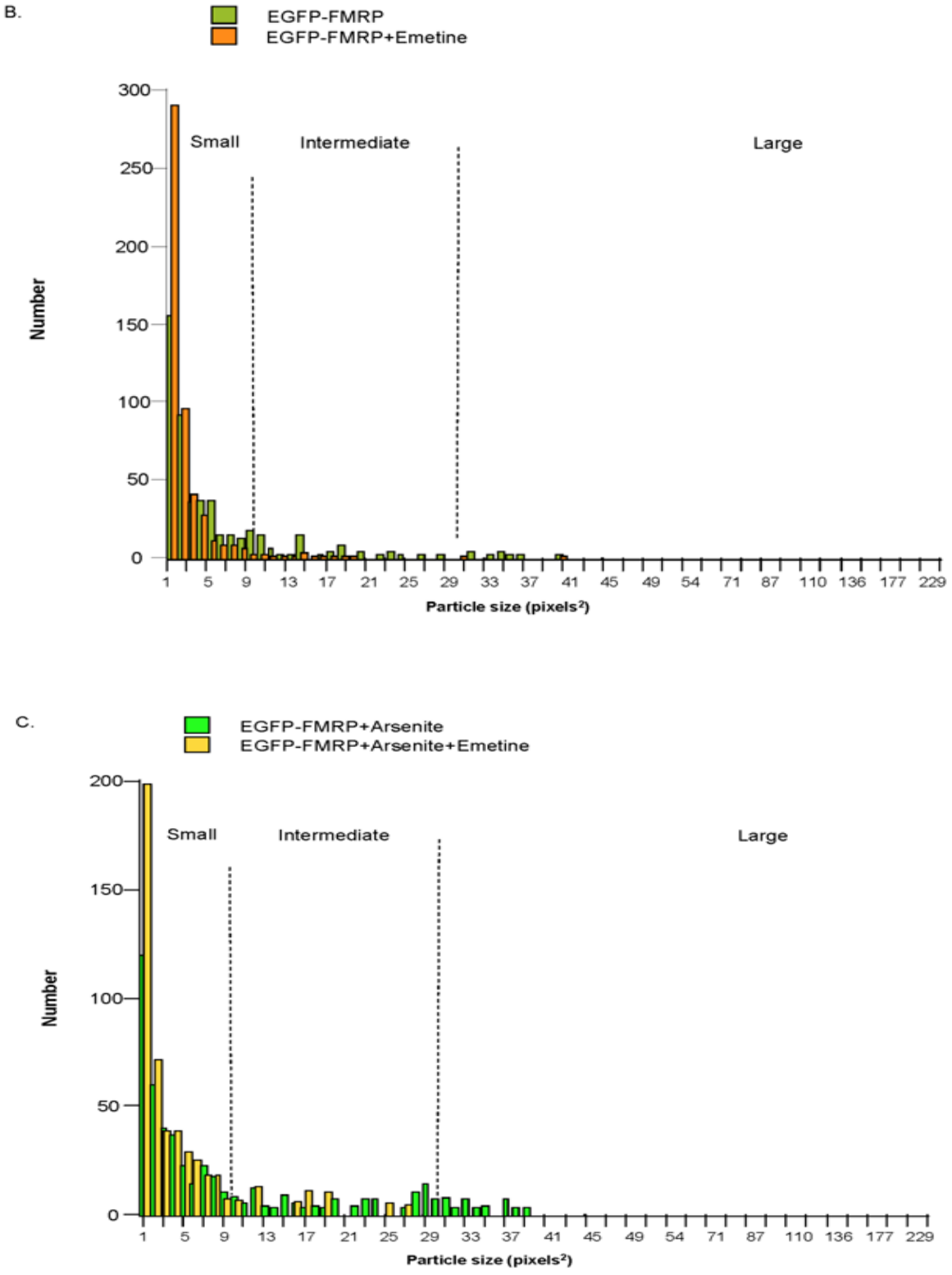

Figure 6. EGFP-FMRP granules respond to emetine. (A) Panels a-d show EGFP-FMRP granules (green) in untreated HeLa cells (a, b) or HeLa cells treated with 0.5 mM arsenite for 20 min or treated with 0.5 mM arsenite and then 10 μg/ml of emetine for 1 h (c, d). All treatments were performed 24 h post-transfection. Boxed areas presented below show magnified views of select stress granules. Size distribution of HeLa cell EGFP-FMRP granules in the absence or presence of emetine and in the (B) absence or (C) presence of arsenite. Analysis was based on 10 transfected cells for each protein. Comparison of the two distributions shows that emetine significantly reduces the size of both classes of stress granules ($P < 0.00084$ and $P < 0.0023$, respectively).

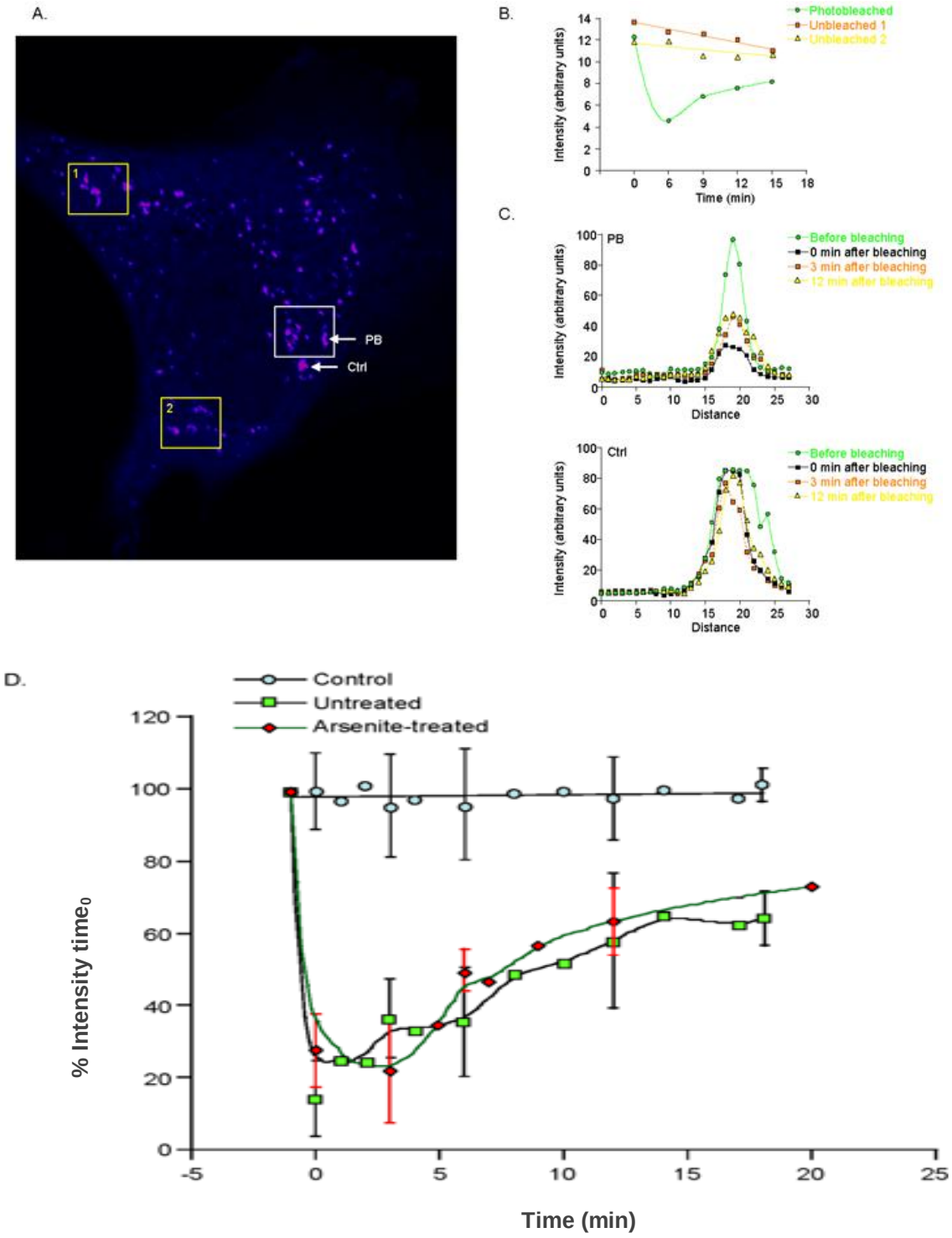

Figure 7. EGFP-FMRP granules are dynamic. (A) Pseudo colored image of EGFP-FMRP expressing HeLa cell. White box shows a region of interest (ROI) prior to photobleaching, while the yellow boxes show comparable ROIs of unbleached EGFP-FMRP granules. Arrows point to a granule that was photobleached (PB) and a nearby control granule (Ctrl) that was not. (B) Time-dependent changes in the intensity of the ROIs shown in (A). (C) Time-dependent changes in PB (upper) and Ctrl (lower) granules shown in (A). (D) Effect of arsenite treatment on EGFP-FMRP photobleaching recovery rates. The intensity at time 0 for 25 non-bleached EGFP-FMRP granules, 23 arsenite-treated photobleached EGFP-FMRP granules and 39 photobleached untreated EGFP-FMRP granules from five different cells was plotted. The difference between the photobleached arsenite-treated granules was not significantly different from the untreated granules ($P > 0.2$, ANOVA). For presentation clarity error bars are shown on every third time point.

or presence of AdOx for twenty-four hours. Subsequently, the cells were immunostained with two antibodies that detect different sets of aDMA proteins. For the untreated cells, cytoplasmic EGFP-FMRP granules exhibited extensive colocalization with the proteins detected by these two antibodies; Figure 8a (panels a-c and f-h). Importantly, AdOx treatment resulted a marked reduction in immunoreactivity, both overall and in the granules, Figure 8a (panels c-e and I-k), indicating that the staining was indeed due to aDMA proteins. Quantitative analyses showed that under the conditions used the extent of the reduction was ca. 50%, Figure 8b.

The aforementioned data suggested that reduced methylation of endogenous proteins does not drastically alter the composition of EGFP-FMRP granules; however, it does not inform one as to whether asymmetric dimethylation affects their formation. To address this question, HeLa cells were pre-treated with AdOx for twenty-four hours prior to transfection. Subsequently, the cells were transfected with the EGFP-FMRP expression vector in AdOx-containing media. As shown in Figure 9a, EGFP-FMRP granules were readily detected even in the continued presence of AdOx implying that full protein methylation is not required for the formation of these granules. In concert with these data treatment with AdOx had no effect on the size distribution of EGFP-FMRP granules (Figure 9b).

We next assessed whether EGFP-FMRP granules contained symmetrically dimethylated (sDMA) proteins. In the absence of treatment we found that the symmetrically dimethylated protein immunoreactivity localized primarily to the nucleus, Figure 10a (panel b). Notably, the cytoplasmic staining partially associated with EGFP-FMRP granules, indicating that these granules are heterogeneous with respect to sDMA-containing proteins, Figure 10b (panel c). However, treating the cells with arsenite following transfection resulted in the recruitment of a significant amount of sDMA proteins into cytoplasmic granules, and in EGFP-FMRP expressing cells; under these conditions almost all of the EGFP-FMRP granules contained sDMA-modified proteins, Figure 10 a and b (panels g-i). Treating the cells with AdOx prior to arsenite treatment significantly decreased the sDMA protein immunoreactivity Figure 10 a and b (panel k), although the extent of colocalization with EGFP-FMRP granules was unchanged, Figure 10b (panels h and k). Consistent with the immunostaining results, Western blot analyses showed that AdOx treatment decreased the amount of aDMA and sDMA in various proteins, albeit to different extents. In contrast, the expression of five different protein arginine methyltransferases (PRMTs) was unaffected by treatment with AdOx (Figure 11).

As these data unequivocally demonstrate sDMA is harbored in arsenite-treated EGFP-FMRP granules we next endeavored to ascertain whether endogenous stress granules also contained sDMA-modified proteins. To this end we treated HeLa cells with arsenite and then immunostained them with antibodies to TIA1 and sDMA. We observed significant colocalization between sDMA-modified proteins and TIA1-containing stress granules (Figure 12).

DISCUSSION

Heterologously expressed EGFP-FMRP has been used as a surrogate marker for endogenous FMRP by several laboratories in a wide variety of studies (Antar et al., 2005; Castren et al., 2001; Cougot et al., 2008; Darnell et al., 2005; Davidovic et al., 2004; De Diego Otero et al., 2002; Dictenberg et al., 2008; Levenga et al., 2009; Pfeiffer and Huber, 2007). Like endogenous FMRP, EGFP-FMRP was found to co-sediment with polyribosomes in cultured neurons (Darnell et al., 2005). Additionally, Antar et al. (2004) showed that EGFP-FMRP was transported to dendrites in the form of granules (Antar et al., 2004). Subsequent work showed that these granules associated with mRNA and kinesin transport motors (Wang et al., 2008) and were responsive to stimulation by the mGluR agonist DHPG. These too are properties of endogenous FMRP (Hou et al., 2006; Kanai et al., 2004).

However, important questions regarding these granules remained to be addressed. Were they uniformly composed? Did they correspond to one or more types of known granules? Could they be modified by various treatments that are known to affect the formation and/or composition of known granule types? Answering these questions in light of the well-established properties of endogenous FMRP granules (Didiot et al., 2008; Dolzhanskaya et al., 2006a, 2006b) was one of the objectives of this study.

In contradistinction to endogenous FMRP granules, which are small and while pervasive in cultured cells not particularly prevalent, (Cougot et al., 2008; Dolzhanskaya et al., 2006a, 2006b) EGFP-FMRP granules are large and amorphous. In fact, they tend to be larger and more non-uniformly round than stress granules (Table 2). Underlying this size/shape heterogeneity we found that EGFP-FMRP granules also are non-uniformly composed. Endogenous FMRP absent environmental stress does not colocalize with stress granule markers; however, in the presence of a stressor such as heat or arsenite FMRP is recruited into stress granules (Didiot et al., 2008; Dolzhanskaya et al., 2006a; Mazroui et al., 2002). Using well-known stress granule markers (TIA1 and FXR1P) we found that EGFP-FMRP granules weakly colocalize with these proteins in the absence of a bonafide stressor; however, stressing EGFP-FMRP-expressing cells with either arsenite or hippuristanol resulted in a marked increase in colocalization, (Figures 2 and 3; Table 1). While the overall colocalization of TIA1 or FXR1P in the absence of stress was low we noticed that in some cells nearly all of the EGFP-FMRP granules

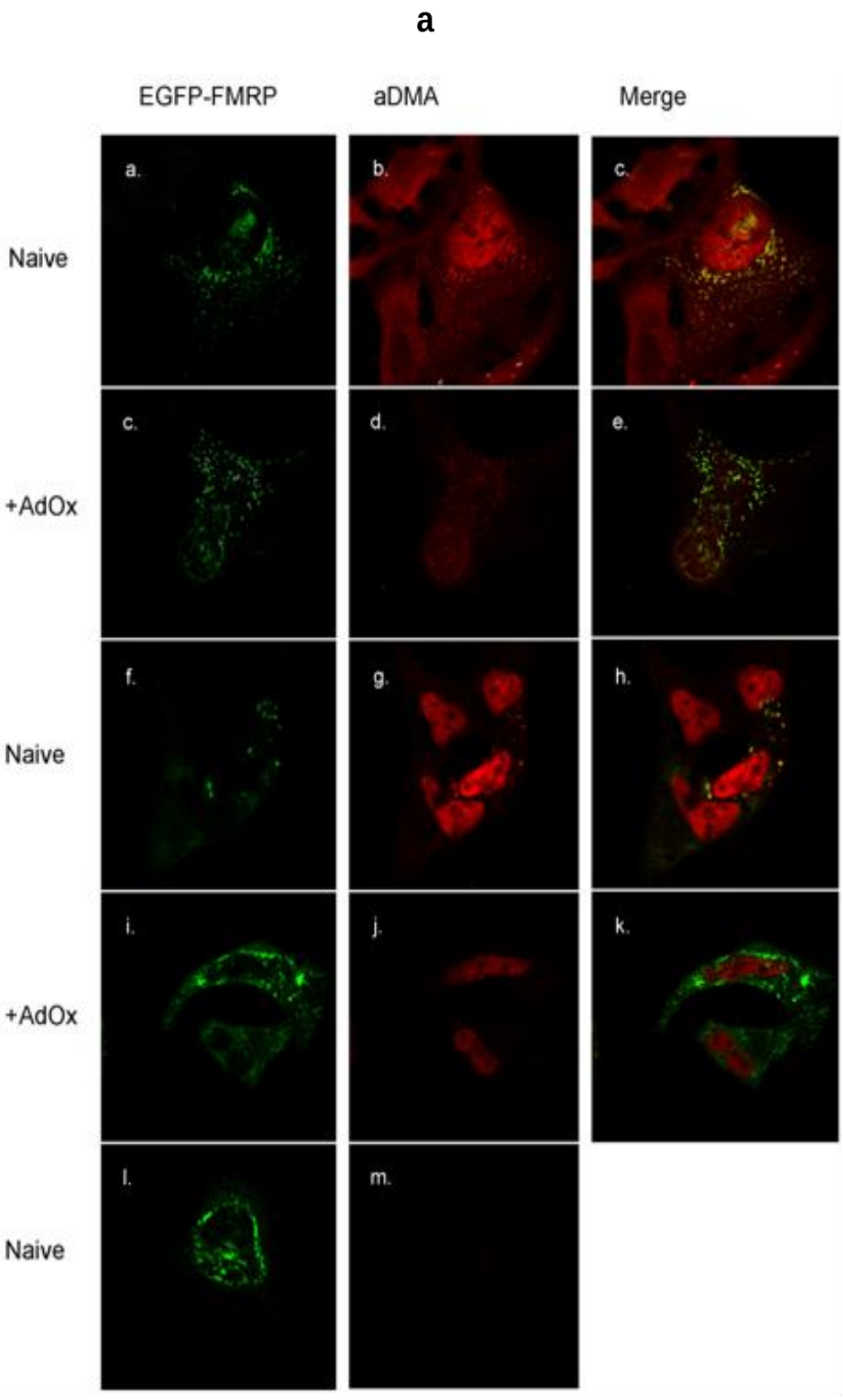

Figure 8A. EGFP-FMRP granules contain asymmetrically dimethylated proteins. (A) HeLa cells expressing EGFP-FMRP were immunostained with antibodies directed to asymmetrically dimethylated proteins. Panels a-e show images of EGFP-FMRP (green), ASYM24 (red), and their merged counterpart whereas panels f-k show images of EGFP-FMRP (green), mRG (red), and their merged counterpart. Panels l-m demonstrate lack of immunostaining in the absence of primary antibody. As indicated, the cells were either treated or not treated with 20 μM AdOx for 24 h following transfection.

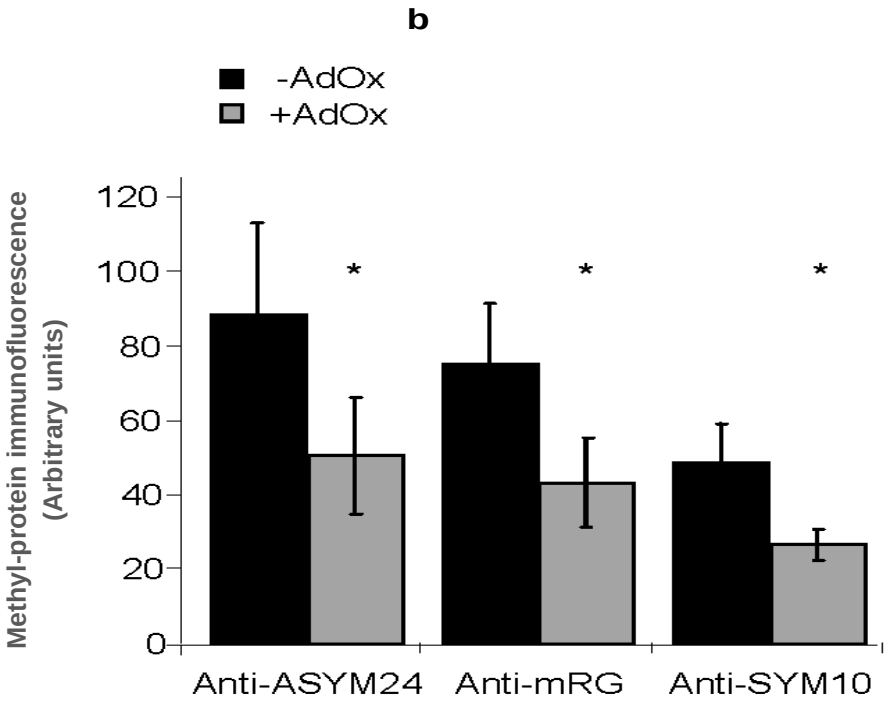

Figure 8B. Quantification of anti-ASYM24 pAb, anti-mRG pAb and anti-SYM10 immunostaining in HeLa cells grown in the absence (-) or presence (+) of 20 μM AdOx. The fluorescence intensity of the individual cells was determined using the histogram function in Adobe Photoshop as previously described (Dolzhanskaya et al., 2006a). The values for 50 - 75 cells/antibody for each treatment are plotted. The reduction in fluorescence intensity in the presence of AdOx was significantly less than in its absence (ASYM24 $P < 5 \times 10\text{-}15$, mRG $P < 4 \times 10^{-15}$, SYM10 $P < 5 \times 10^{-17}$ ANOVA).

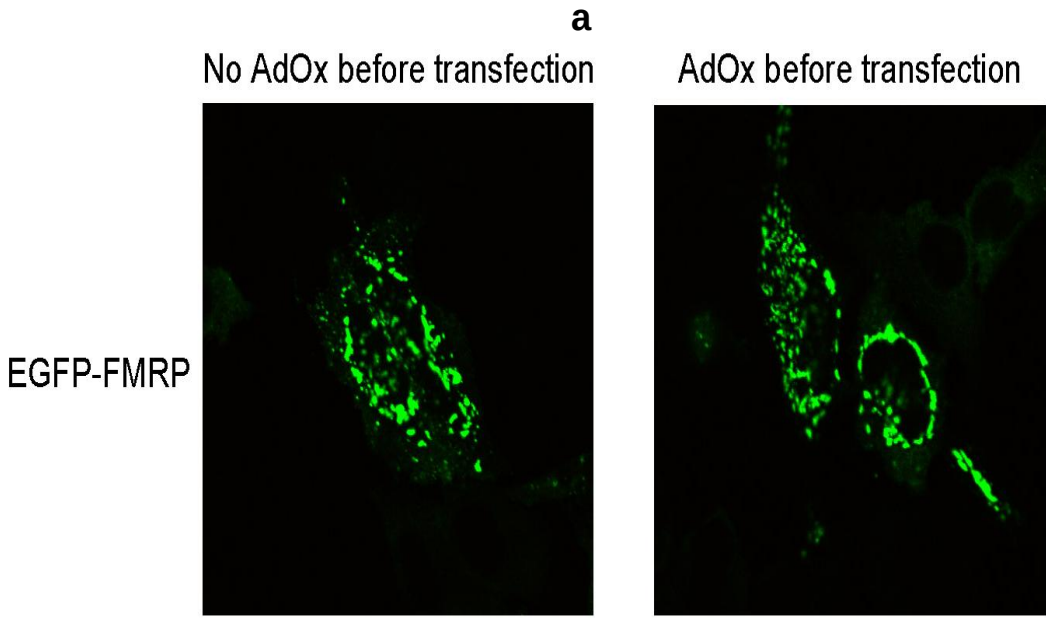

Figure 9A. EGFP-FMRP granule expression does not require full protein methylation. (A) HeLa cells were either treated or not treated with 20 μM AdOx for 24 h prior to transfection. Subsequently, the cells were transfected with pEGFP-FMRP and imaged 24 h later. Note: AdOx was re-applied to the set of cells that were pre-treated with AdOx.

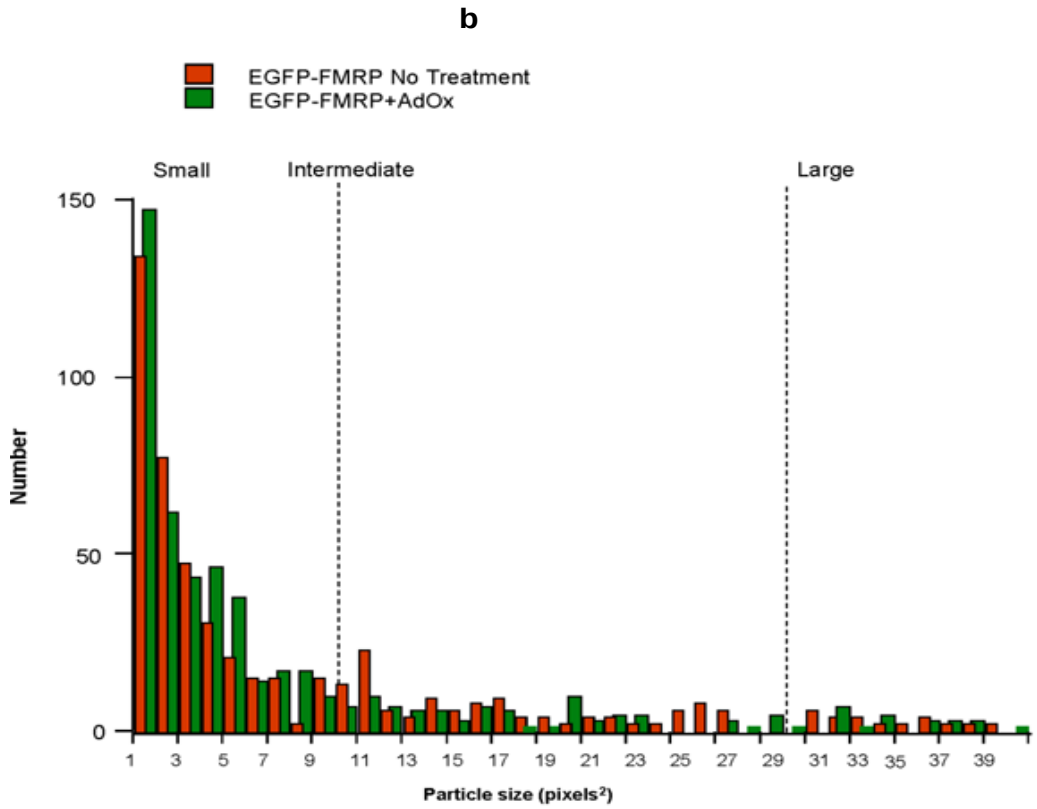

Figure 9B. Size distribution of HeLa cell arsenite-treated EGFP-FMRP granules in the presence and absence of AdOx. Analysis was based on 10 transfected cells/treatment. Comparison of the two distributions shows that AdOx does not significantly reduce the size of EGFP-FMRP granules (P > 0.4).

colocalized with these markers. Currently, the molecular and cellular basis of this phenomenon is unknown. It may be related in some way to the cell cycle or it may simply be a stochastic phenomenon and we are investigating these possibilities. More importantly however, the data demonstrate that EGFP-FMRP granules are biochemically heterogeneous and this non-uniformity must be considered when interpreting studies that use these granules as markers.

Contradicting data exists regarding the association of FMRP with P-bodies. Several lines of evidence have shown that FMRP, or its *Drosophila* counterpart dFMR1, interact specifically with components that are associated with P-bodies (Anderson and Kedersha, 2006). Ishizuka et al. (2002) first demonstrated that dFMR1 interacted with Ago2 and the RNA helicase Dmp68 (Ishizuka et al., 2002); more recently Cheever et al showed that FMRP interacts with Dicer in a phosphorylation-dependent fashion (Cheever and Ceman, 2009). Moreover, immunofluorescence studies showed that endogenous FMRP partially overlapped the staining of both Ago3 and Ago4 in rat dorsal root ganglion (DRG) processes (Hengst et al., 2006), while EGFP-FMRP and GFP-dFMR1 colocalized with Dcp1 (Barbee et al., 2006; Cougot et al., 2008). Nevertheless, Didiot et al. (2008) failed to observe much localization of endogenous FMRP with Dcp1a in HeLa cells (Didiot et al., 2008). Here we found a weak colocalization between EGFP-FMRP granules and the P-body marker Dcp1a, Figure 6 and Table 1. We hypothesize that the differing results may be related to differences in the species and tissue expression of P-body components (González-González et al., 2008) and in the heterogeneity of Ago-containing granules (González-González et al., 2008; Iwasaki et al., 2009).

We also investigated whether EGFP-FMRP granules were in dynamic equilibrium with polyribosomes and/or the pool of non-granular cytoplasmic EGFP-FMRP by emetine treatment (Kedersha et al., 2000) and FRAP (Lippincott-Schwartz et al., 1999), respectively. Here we found that EGFP-FMRP granules mimic the properties of endogenous FMRP, implying that there are certain “core characteristics” of granules that are invariant (Buchan and Parker, 2009).

Large ribonucleoprotein granules are often regulated by one or more post-translational modifications (Qi et al., 2008; Yoon et al., 2010). Stress granules, in particular, undergo a myriad of such reactions (Carpio et al., 2010;

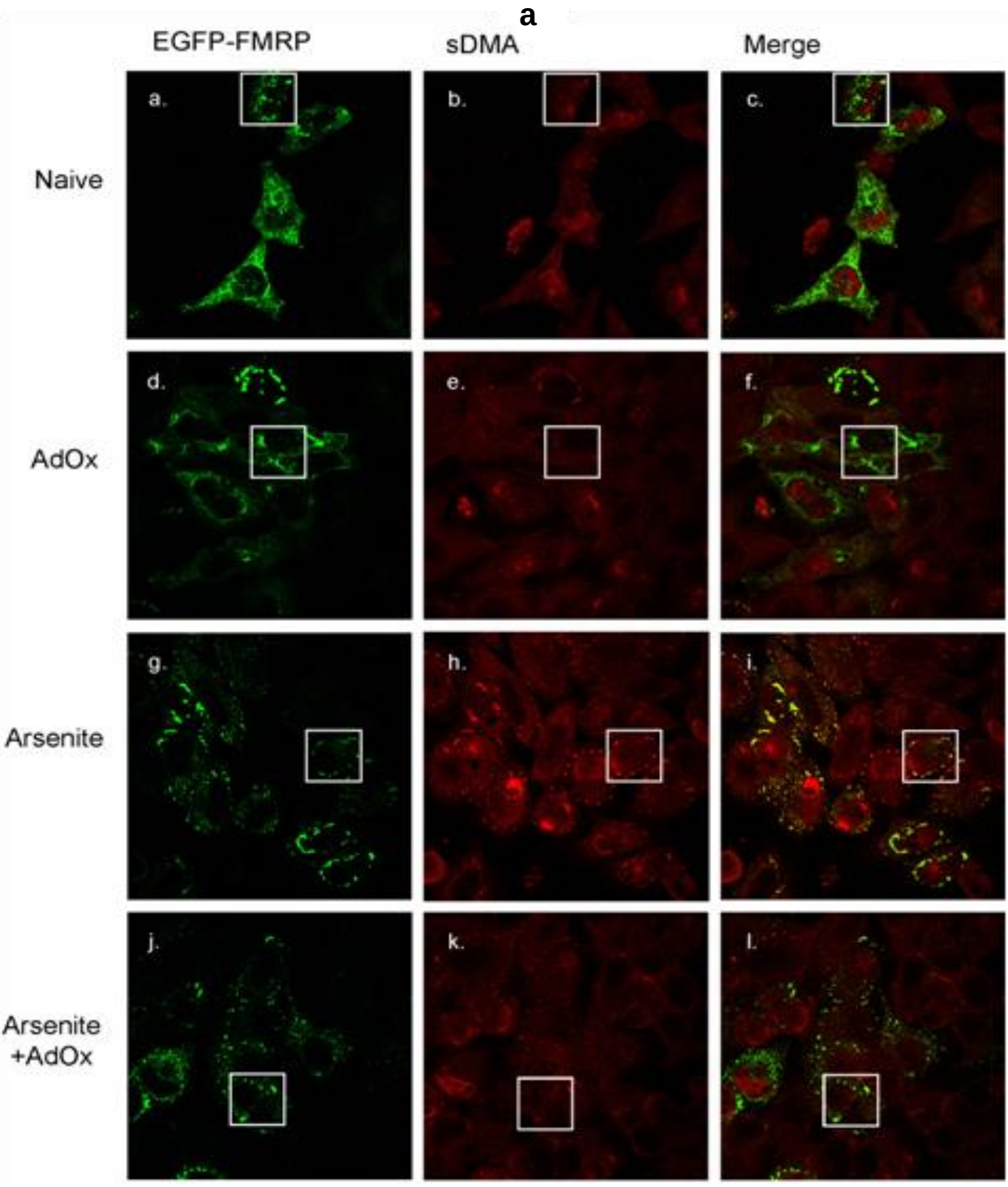

Figure 10A. EGFP-FMRP granules contain symmetrically dimethylated proteins. (A) HeLa cells expressing EGFP-FMRP were immunostained with an antibody directed to symmetrically dimethylated proteins (sDMA), SYM10. Panels a-f show images of EGFP-FMRP (green), sDMA (red), and their merged counterparts in untreated cells and cells treated with 20 μM AdOx for 24 h following transfection. Panels g-l show cells comparably treated cells that were either treated or not treated with 0.5 mM arsenite for 20 min, 24 h post-transfection.

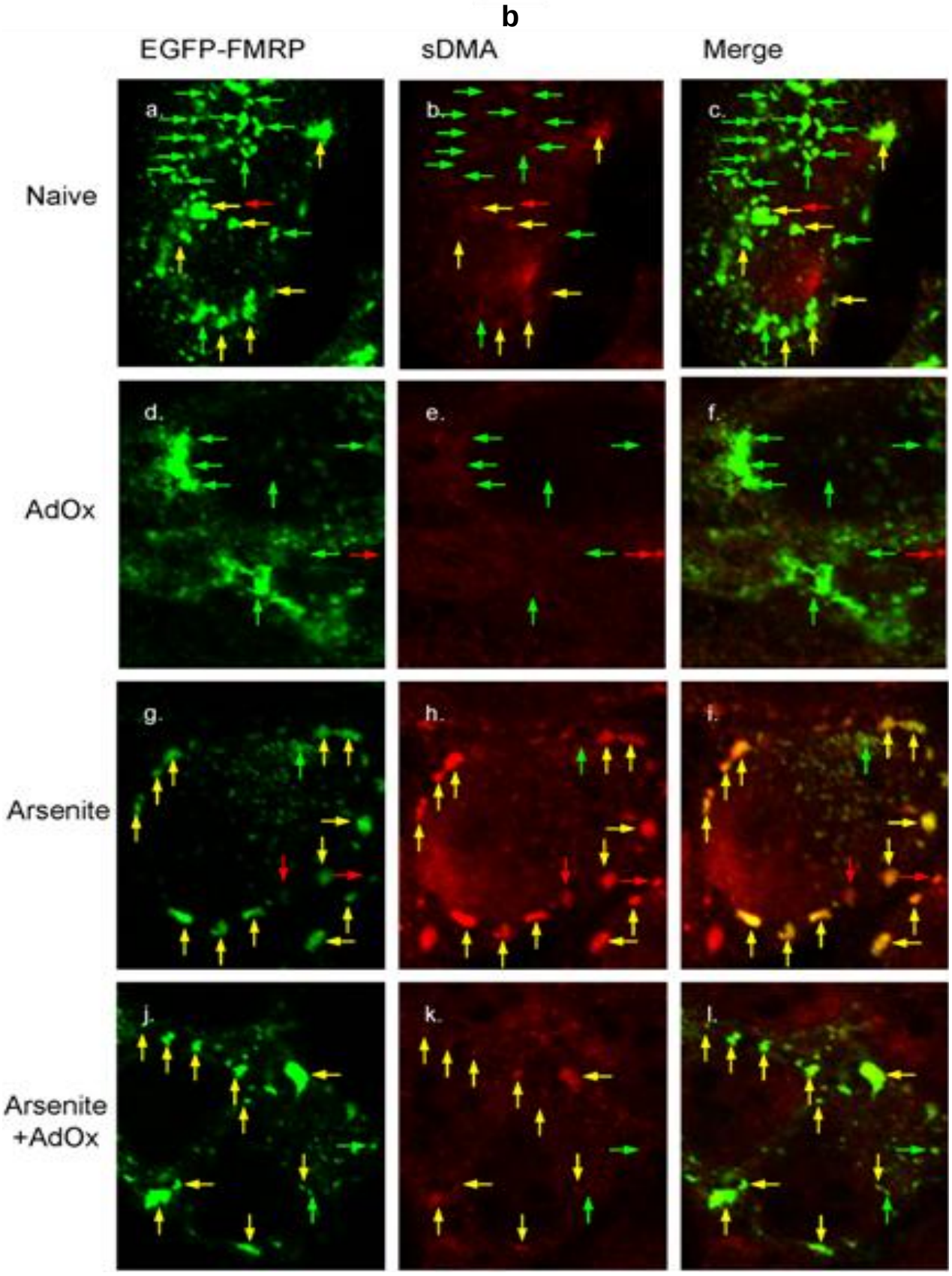

Figure 10B. Boxed areas from (A) show magnified views of select cells; yellow arrows mark colocalizing granules, green arrows mark EGFP-FMRP only granules and red arrows mark sDMA only granules.

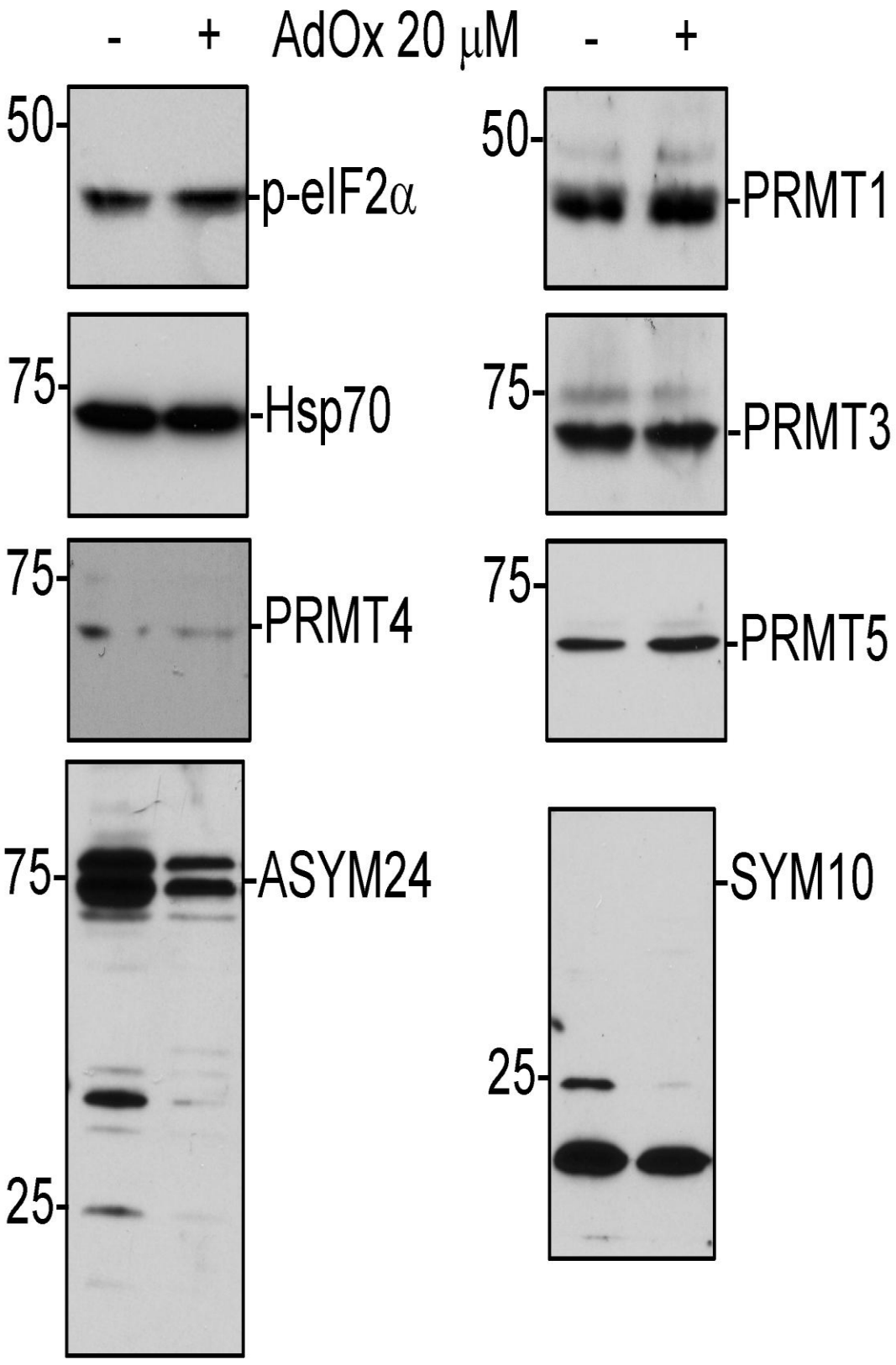

Figure 11. AdOx inhibits cellular methylation of proteins that colocalize in EGFP-FMRP granules. Representative Western blots of HeLa cell proteins (30 μg) probed with antibodies directed to methylated proteins, ASYM24 pAb (left) and SYM10 pAb (right), protein arginine methyltransferases (PRMTs) 1, 3, 4, and 5 and various load controls.

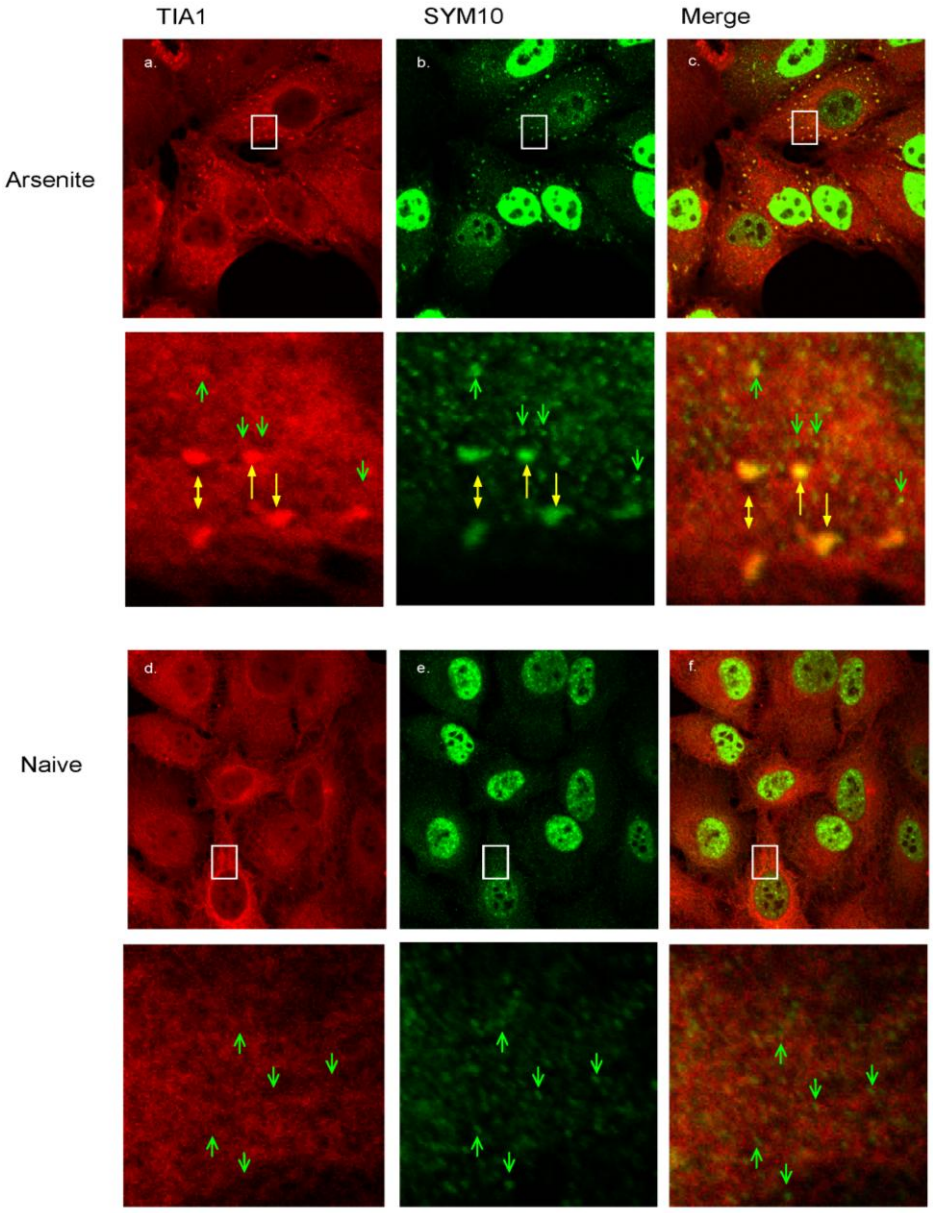

Figure 12. Endogenous TIA1 stress granules contain sDMA proteins. HeLa cells were treated with 0.5 mM sodium arsenite (panels a-c) or not treated panels (d-f). Subsequently, the cells were immunostained with antibodies that detect the stress granule marker TIA1 (red) and SYM10 (green) and subject to confocal microscopy. Magnified views of select regions of the upper panels are presented below to clearly show the granules. Large TIA1-containing stress granules that colocalize with symmetrically dimethylated proteins are marked with yellow arrows. These are contrasted with smaller granules harboring symmetrically dimethylated proteins, but which do not colocalize with TIA1 (green arrows). Note that these smaller granules are constitutively present in untreated cells. We speculate that these may be related to the 7S PRMT5 complex, the 20S methylosome or the SMN complex.

Kwon et al., 2007; Mazroui et al., 2007; Wasserman et al., 2009), among which is protein arginine methylation. We have previously demonstrated that native stress granules contain asymmetrically dimethylated (aDMA) proteins and that pharmacological inhibition of protein methylation altered their FXR1P content; in contrast, endogenous FMRP granules were devoid of aDMA-containing proteins (Dolzhanskaya et al., 2006a). Thus, it was of interest to determine whether EGFP-FMRP granules associated with methylated proteins and if so

what role they played in granule formation. We found that EGFP-FMRP granules, like stress granules, always contained aDMA- modified proteins and sometimes contained sDMA-modified proteins, Figure 8 and Figure 10a, b (panel c). Interestingly, we also determined that endogenous stress granules harbored sDMA-containing proteins and because the sDMA antibody used overwhelmingly recognizes splicing-related proteins (Boisvert et al., 2003) these data provide a potential link between mRNA splicing and stress granules. Future studies must address the identities of the sDMA-containing proteins to confirm this connection. Finally, using AdOx to significantly reduce endogenous protein methylation we discovered that protein methylation is not required for the formation of EGFP-FMRP granules, Figure 9. Thus, although methylation clearly can affect protein dimerization (Dolzhanskaya, 2006a) it appears less intimately involved in the assembly/disassembly of granules than phosphorylation, deacetylation and ubiquitination.

Overall, our work has shown both similarities and marked differences between EGFP-FMRP granules and three defined granule types: endogenous FMRP granules, stress granules and P-bodies. The fact that EGFP-FMRP granules uniformly contain aDMA-modified proteins distinguishes them from endogenous FMRP granules. Thus, EGFP-FMRP is not an appropriate surrogate for FMRP, and studies that have used it as a marker may need to be reinterpreted in light of this new information. Additionally, because of the weak overlap with stress granule and P-body markers the vast majority of EGFP-FMRP is not normally present in stress granules or P-bodies. However, triggering stress granule and P-body formation with arsenite (Kedersha et al., 2007), or stress granule formation with hippuristanol (Mazroui et al., 2006) resulted in the near-complete recruitment of EGFP-FMRP into stress granules, Figures 2 and 3. Thus, these data are consistent with the view that EGFP-FMRP granules are uniquely poised to become stress granules; hence, we have called them proto-stress granules.

ACKNOWLEDGEMENTS

We thank Drs. Ying-Ju Sung and W. Ted Brown for helpful discussions concerning this manuscript. These studies were generously supported by the New York State Research Foundation for Mental Hygiene and the FRAXA Research Foundation.

REFERENCES

Anderson P, Kedersha N (2006). RNA granules. J. Cell Biol., 172: 803-808.

Antar LN,Afroz R,Dictenberg J, BCarroll RC, Bassell GJ (2004). Metabotropic glutamate receptor activation regulates fragile X mental retardation protein and Fmr1 mRNA localization differentially in dendrites at synapses. J. Neurosci., 24: 2648.

Antar LN, Dictenberg JB, Plociniak M, Afroz R, Bassell GJ (2005). Localization of FMRP-associated mRNA granules requirement of microtubules for activity-dependent trafficking in hippocampal neurons. Genes Brain Behav., 4: 350.

Aschrafi A ,Cunningham BA , Edelman GM , Vanderklish PW (2005). The fragile X mental retardation protein and group I metabotropic glutamate receptors regulate levels of mRNA granules in brain. Proc. Nat'l Acad. Sci., 102: 2180.

Barbee SA, Estes PS, Cziko AM, Hillebrand J, Luedeman RA, Coller JM, Johnson N, Howlett IC, Geng C, Ueda R (2006). Staufen FMRP-containing neuronal RNPs are structurally and functionally related to somatic P bodies. Neuron, 52: 997.

Bassell GJ , Warren ST (2008). Fragile X syndrome: Loss of local mRNA regulation alters synaptic development function, 60: 201.

Biron VL, McManus KJ, Hu N, Hendzel MJ, Underhill DA(2004). Distinct dynamics distribution of histone methyl-lysine derivatives in mouse development. Dev. Biol., 276: 337

Bloch DB, Nobre R (2010). p58TFL does not localize to messenger RNA processing bodies Letter. Mol. Cancer Res., 8(131).

Boisvert FM, Cote J, Boulanger MC, Richard S(2003). A proteomic analysis of arginine methylated protein complexes. Mol. Cell Proteomics, 2: 1319.

Bolte S, Cordelieres FP. (2006). A guided tour into subcellular colocalization analysis in light microscopy J. Microsc., 224: 213.

Brand A (1999). GFP as a cell developmental marker in the Drosophila nervous system In Green Fluroescent Proteins vol. 58 eds KF, Sullivan S A, Kay San Diego, Academic Press, pp. 165-180.

Buchan JR, Parker R (2009). Eukaryotic stress granules: The ins and outs of translation. Mol Cell, 36: 932-941.

Carpio MA, LÃ³pezÂ Sambrooks C,Durand ES, Hallak ME (2010). The arginylation-dependent association of calreticulin with stress granules is regulated by calciu. Biochem. J., 429: 63-72.

Castren M, Haapasalo A, Oostra B,Castren E (2001). Subcellular localization of fragile X mental retardation protein with the I304N mutation in the RNA-binding domain in cultured hippocampal neurons .Cell. Mol. Neurobiol., 21: 29

Cheever A, Ceman S (2009). Phosphorylation of FMRP inhibits association with Dicer. RNA, 15: 362

Cougot N, Babajko S, Seraphin B (2004). Cytoplasmic foci are sites of mRNA decay in human cells. Cell. Mol. Neurobiol., 165: 31

Cougot N, Bhattacharyya SN,Tapia-Arancibia L,Bordonne R, Filipowicz W, Bertrand E, Rage F (2008). Dendrites of mammalian neurons contain specialized P-body-like structures that respond to neuronal activation. J. Neurosci., 28: 13793-13804.

Cziko AMJ, McCann CT, Howlett IC, Barbee SA, Duncan RP, Luedemann R, Zarnescu D, Zinsmaier KE, Parker RR, Ramaswami M (2009). Genetic modifiers of dFMR1 encode RNA-granule components in Drosophila. Genetics, 182:1051-1060.

Darnell, JC, Mostovetsky O, Darnell RB (2005). FMRP RNA targets: identification and validation. Genes Brain Behav., 4: 341-349.

Davidovic L, Huot MC, Khandjian E. (2004). Lost once, the fragile X mental retardation protein is now back on brainpolyribosomes. RNA Biol., 1: 125-127.

B,Willemsen R (2002). Transport of fragile X mental retardation proteinvia granules in neurites of PC12 Cells. Mol. Cell. Biol., 22: 8332-8341.

Detrich III HW (2008). Fluorescent proteins in zebrafish cell and developmental biology. In Fluorescent Proteins (ed. KF. Sullivan), San Diego: Academic Press, 85: 220-237.

Di Giorgi F, Ahmed Z, Bastianutto C, Brini M, Jouaville S, Marsault R,Murgia M,Pinton P,Pozzan T,Rizzuto R (1999). Targeting GFP to organelles. In Green Fluroescent Proteins (eds K F Sullivan ,SA Kay), San Diego: Academic Press, 58: 75-85.

Dictenberg JB, Swanger SA, Antar LN, Singer RH, Bassell GJ (2008). A direct role for FMRP in activity-dependent dendritic mRNA transport links filopodial-spine morphogenesis to fragile X syndrome. Dev. Cell, 14: 926-939.

Didiot MC, Subramanian M, Flatter E Mandel JL, Moine H (2008). Cells lacking the fragile X mental retardation protein (FMRP) have normal RISC activity but exhibit altered stress granule assembly. Mol. Biol. Cell, 20: 428-437.

Dolzhanskaya N, Merz G, Aletta JM, Denman RB (2006a). Methylation

regulates FMRP's intracellular protein-protein and protein-RNA interactions. J. Cell. Sci., 119: 1933-1946.
Dolzhanskaya N, Merz G, Denman RB (2006b). Oxidative stress reveals heterogeneity of FMRP granules in PC12 cell neurites. Brain Res., 1112: 56-64.
Encinas, JM, Enikolpov G (2008). Identifying and quantifying neural stem cell and progenitor cells in the adult brain. In Fluorescent Proteins (ed. KF Sullivan), San Diego: Academic Press, 85: 244-270.
Gay DA, Sisodia SS, Cleveland DW (1989). Autoregulatory control of beta-tubulin mRNA stability is linked to translation elongation. Proceedings of the National Academy of Sciences of the United States of America, 86: 5763-5767.
González-González E, López-Casas PP, del Mazo J (2008). The expression patterns of genes involved in the RNAi pathways are tissue-dependent and differ in the germ and somatic cells of mouse testis. Biochim. Biophys. Acta (BBA) - Gene Regulatory Mechanisms, 1779: 306-311.
Grollman AP, Huang MT (1976). Protein Synthesis. New York: Marcel Dekker.
Hengst U, Cox LJ, Macosko EZ, Jaffrey SR (2006). Functional and selective RNA interference in developing axons and growth cones. J. Neurosci., 26: 5727-5732.
Hou L, Antion MD, Hu D, Spencer CM, Paylor R, Klann E (2006). Dynamic translational and proteasomal regulation of fragile X mental retardation protein controls mGluR-dependent Long-Term Depression. Neuron, 51: 441-454.
Ishizuka A, Siomi MC, Siomi H (2002). A Drosophila fragile X protein interacts with components of RNAi and ribosomal proteins. Genes Dev., 16: 2497-508.
Iwasaki S, Kawamata T, Tomari Y (2009). Drosophila Argonaute1 and Argonaute2 employ distinct mechanisms for translational repression. Mol. Cell, 34: 58-67.
Kanai Y, Dohmae N, Hirokawa N (2004). Kinesin transports RNA: isolation and characterization of an RNA-transporting granule. Neuron, 43: 513-525.
Kedersha N, Anderson P, Jon L (2007). Mammalian stress granules and processing bodies. In Methods in Enzymology, Academic Press, 431: 61-81.
Kedersha N, Cho MR, Li W, Yacono PW, Chen S, Gilks N, Golan DE Anderson P (2000). Dynamic shuttling of TIA-1 accompanies the recruitment of mRNA to mammalian stress granules. J. Cell Biol., 151: 1257-1268.
Kedersha N, Stoecklin G, Ayodele M, Yacono P, Lykke-Andersen J Fitzler MJ, Scheuner D, Kaufman RJ, Golan DE Anderson P (2005). Stress granules and processing bodies are dynamically linked sites of mRNP remodeling. J. Cell Biol., 169: 871-884.
Kedersha N, Tisdale S, Hickman T, Anderson P, Maquat LE, Kiledjian M (2008). Real-time and quantitative imaging of mammalian stress granules and processing bodies. In Methods in Enzymology. Academic Press, 448: 521-552.
Kwon S,Zhang Y, Matthias P (2007). The deacetylase HDAC6 is anovel critical component of stress granules involved in the stress response. Genes Dev., 21: 3381-3394.
Levenga J, Buijsen RAM, Rifé M, Moine H, Nelson DL, Oostra BA, Willemsen R, de Vrij FMS (2009). Ultrastructural analysis of the functional domains in FMRP using primary hippocampal mouse neurons. Neurobiol. Dis., 35:241-250.
Ling SC, Fahrner PS, Greenough WT, Gelfand VI (2004). Transport of
Drosophila fragile X mental retardation protein-containing ribonucleoprotein granules by kinesin-1 and cytoplasmic dynein. Proc Nat'l Acad. Sci., 101: 17428.
Lippincott-Schwartz J, Presley F, Zaal KJM, Hirschberg K, Miller CD Ellenberg J(1999). Monitoring the dynamics of membrane proteins tagged with green fluorescent protein. In Green Fluroescent Proteins vol. 58 eds KF, Sullivan SA, Kay San Diego: Academic Press, pp. 261-280.
Mazroui R, Di Marco S, Kaufman RJ, Gallouzi IE (2007). Inhibition of the ubiquitin-proteasome system induces stress granule formation. Mol. Biol. Cell, 18: 2603-2618.
Mazroui R, Huot ME, Tremblay S, Filion C, Labelle Y, Khandjian EW. (2002). Trapping of messenger RNA by fragile X mental retardation protein into cytoplasmic granules induces translation repression. Hum. Mol. Genet., 11: 3007-3017.
Mazroui R, Sukarieh R, Bordeleau ME, Kaufman RJ, Northcote P, Tanaka J, Gallouzi I, Pelletier J (2006). Inhibition of ribosome recruitment induces stress granule formation independent of eIF2{alpha} phosphorylation. Mol. Biol. Cell, 17: 4212-4219.
McEwen E, Kedersha N, Song B, Scheuner D, Gilks N, Han A, Chen JJ, Anderson P, Kaufman RJ (2005). Heme-regulated inhibitor kinase-mediated phosphorylation of eukaryotic translation initiation factor 2 inhibits translation, induces stress granule formation, and mediates survival upon arsenite exposure. J. Biol. Chem., 280: 16925-16933.
Minagawa K, Katayama Y, Nishikawa S, Yamamoto K, Sada A, Okamura A, Shimoyama M, Matsui T (2009). Inhibition of G1 to S phase progression by a novel zinc finger protein p58TFL at P-bodies. Mol. Cancer Res., 7: 880-889.
Minagawa K, Matsui T (2010). p58TFL does not localize to messenger RNA processing bodies - Response. Mol. Cancer Res., 8: 132-133.
Özlü N, Srayko M, Kinoshita K, Habermann BO ,Toole ET, Müller-Reichert T, Schmalz N, Desai A, Hyman AA (2005). An essential function of the C. elegans ortholog of TPX2 is to localize activated Aurora A kinase to mitotic spindles. Dev. Cell, 9: 237-248.
Pfeiffer BE, Huber KM (2007). Fragile X mental retardation protein induces synapse loss through acute postsynaptic translational regulation. J. Neurosci., 27: 3120-3130.
Pierce D, Vale RD (1999). Single-molecule fluorescence detection of green fluorescent protein and application to single protein dynamics. In Green Fluroescent Proteins (eds KF,Sullivan SA, Kay, San Diego: Academic Press, 58: 49-72.
Qi HH, Ongusaha PP, Myllyharju J, Cheng D, Pakkanen O, Shi Y, Lee SW, Peng J, Shi Y (2008). Prolyl 4-hydroxylation regulates Argonaute 2 stability. Nature, 455: 421-424.
Querido E, Chartrand P (2008). Using fluorescent proteins to study mRNA trafficking in living cells. In Fluorescent Proteins (ed. KF Sullivan), San Diego: Academic Press, 85: 274-291.
Rackham O, Brown CE (2004). Visualization of RNA-protein interactions in living cells: FMRP and IMP1 interact on mRNAs. EMBO J., 23: 3346-3355.
Solomon S, Xu Y, Wang B, David MD, Schubert P, Kennedy D, Schrader JW (2007). Distinct structural features of caprin-1 mediate its interaction with G3BP-1 and its induction of phosphorylation of eukaryotic translation initiation factor 2{alpha}, entry to cytoplasmic stress granules, and selective interaction with a subset of mRNAs. Mol. Cell Biol., 27: 2324-2342.
Thomas MG, Martinez Tosar LJ, Loschi M, Pasquini JM, Correale J, Kindler S, Boccaccio GL (2004). Staufen recruitment into stress granules does not affect early mRNA transport in oligodendrocytes. Mol. Biol. Cell, 16: 405-420.
Wang H, Dictenberg JB, Ku L, Li W, Bassell GJ, Feng Y (2008). Dynamic association of the fragile X mental retardation protein as a messenger ribonucleoprotein between microtubules and polyribosomes. Mol. Biol. Cell, 19: 105-114.
Wasserman T, Katsenelson K, Daniliuc S, Hasin T, Choder M, Aronheim A(2009). A novel JNK binding protein WDR62 is recruited to stress granules and mediates a non-classical JNK activation. Mol. Biol. Cell, 21: 117-130.
Xie W, Dolzhanskaya N, LaFauci G, Dobkin C, Denman RB (2009). Tissue and developmental regulation of fragile X mental retardation protein exon 15 isoforms. Neurobiol. Dis., 35: 52-62.
Yamasaki S, Stoecklin G, Kedersha N, Simarro M, Anderson P (2007). T-cell intracellular antigen-1 (TIA-1)-induced translational silencing promotes the decay of selected mRNAs. J. Biol. Chem., 282: 30070-30077.
Yoon JH, Choi EJ, Parker R (2010). Dcp2 phosphorylation by Ste20 modulates stress granule assembly and mRNA decay in *Saccharomyces cerevisiae*. J. Cell Biol., 189: 813-827.